

1 Image-based surface reconstruction in geomorphometry – 2 merits, limits and developments ~~of a promising tool for~~ 3 **geoscientists**

4
5 **A. Eltner¹, A. Kaiser², C. Castillo³, G. Rock⁴, F. Neugirg⁵ and A. Abellan⁶**

6 [1] {Institute of Photogrammetry and Remote Sensing, Technical University Dresden,
7 Germany}

8 [2] {Soil and Water Conservation Unit, Technical University Freiberg, Germany}

9 [3] {Dep. of Rural Engineering, University of ~~Córdoba~~Córdoba, Spain}

10 [4] {Dep. of Environmental Remote Sensing and Geomatics, University of Trier, Germany}

11 [5] {Dep. of Physical Geography, Catholic University Eichstätt-Ingolstadt, Germany}

12 [6] {Risk Analysis Group, Institute of Earth Sciences, University of Lausanne, Switzerland}

13 Correspondence to: A. Eltner (Anette.Eltner@tu-dresden.de)

14 15 **Abstract**

16 Photogrammetry and geosciences ~~are~~have been closely linked since the late 19th century-
17 ~~Today, a wide range of commercial and open-source software enable non-experts users due~~ to
18 ~~obtain~~the acquisition of high-quality 3D datasets of the environment, ~~which was formerly~~
19 ~~reserved~~but it has so far been restricted to a limited range of remote sensing ~~experts,~~
20 ~~geodesists or owners of~~specialists because of the considerable ~~cost-intensive of~~
21 systems for the acquisition and treatment of airborne ~~imaging systems. Complex~~
22 ~~tridimensional~~imagery; Nowadays, a wide range of commercial and open-source software
23 tools enable the generation of 3D and 4D models of complex geomorphological features ~~can~~
24 ~~be easily reconstructed from images captured with consumer grade cameras. Furthermore, by~~
25 geoscientists and other non-experts users. In addition, very recent rapid developments in
26 unmanned aerial vehicle (UAV) technology allow forallows for the flexible generation of
27 high quality aerial surveying and orthophotography ~~generation~~ at a relatively low-cost.

28 The increasing computing ~~capacities~~capabilities during the last decade, together with the
29 development of high-performance digital sensors and the important software innovations
30 developed by ~~other fields of research (e.g. computer~~ based vision and visual perception)

1 [research fields](#) has extended the rigorous processing of stereoscopic image data to a 3D point
2 cloud generation from a series of non-calibrated images. Structure from motion ~~methods offer~~
3 ~~algorithms, e.g. robust feature detectors like the scale-invariant feature transform for 2D~~
4 ~~imagery, which allow~~(SfM) workflows are based upon [algorithms](#) for efficient and automatic
5 orientation of large image sets without further data acquisition information. ~~examples~~
6 ~~including robust feature detectors like the scale-invariant feature transform for 2D-imagery.~~
7 Nevertheless, the importance of carrying out ~~correct~~[well-established](#) fieldwork strategies,
8 using proper camera settings, ground control points and ground truth for understanding the
9 different sources of errors still need to be adapted in the common scientific practice.

10 This review ~~manuscript~~ intends not only to summarize the ~~present~~[current](#) state of ~~published~~
11 ~~research~~[the art](#) on ~~structure from motion photogrammetry applications using SfM workflows~~
12 in geomorphometry, but also to give an overview of terms and fields of application. ~~Further~~
13 ~~this article aims~~ to quantify already achieved accuracies and used scales using different
14 strategies, to evaluate possible stagnations of current developments and to identify key future
15 challenges. It is our belief that ~~some lessons learned in already published articles, scientific~~
16 ~~reports and book chapters concerning~~ the identification of common errors, ~~or~~ “bad practices”
17 and some other valuable information ~~in already published articles, scientific reports and book~~
18 ~~chapters~~ may help in guiding the future use of SfM photogrammetry in geosciences.

20 **1 Introduction**

21 Early works on projective geometries date back to more than five centuries, when scientists
22 derived coordinates of points from several images and investigated the geometry of
23 perspectives. Projective geometry represents the basis for the developments in
24 photogrammetry in the late 19th century, when Aimé Laussedat experimented with terrestrial
25 imagery as well as kites and balloons for obtaining imagery for topographic mapping
26 (Laussedat, 1899). Rapidly, photogrammetry advanced to be an essential tool in geosciences
27 during the last two decades and is lately gaining momentum driven by digital sensors.
28 Simultaneously, growing computing capacities and rapid developments in computer vision
29 ~~lead~~[led](#) to the ~~promising~~ method of Structure from Motion (SfM) that opened the way for low-
30 cost high-resolution topography. Thus, the community using image-based 3D reconstruction
31 experienced a considerable growth, not only in quality and detail of the achieved results but
32 also in the number of potential users from diverse geo-scientific disciplines.

1 SfM photogrammetry can be performed with images acquired with consumer grade digital
2 cameras and is thus very flexible in its implementation. Its ease of use in regard to data
3 [acquisition and](#) processing makes it further interesting to non-experts- [\(Fig. 1\)](#). The diversity
4 of possible applications led to a variety of terms used to describe SfM photogrammetry either
5 from photogrammetric or computer vision standpoint. Thus to avoid ambiguous terminology,
6 a short list of definitions in regard to the reviewed method is given in Table 1. In this review a
7 series of studies that utilise the algorithmic ~~advances~~[advance](#) of [high automation in](#) SfM
8 are considered, i.e. no initial estimates [of the image network geometry](#) or user interactions to
9 generate initial estimates are needed. Furthermore, data processing ~~is~~[can be](#) performed [almost](#)
10 fully automatic-~~but~~. ~~However, some~~ parameter settings, typical for photogrammetric tools,
11 [\(e.g. camera calibration values\)](#), can be applied to optimise both accuracy and precision, [and](#)
12 [GCP or scale identification are still necessary](#).

13 SfM photogrammetry can be applied to a vast range of temporal as well as spatial scales and
14 resolutions up to an unprecedented level of detail, allowing for new insights into earth surface
15 processes, i.e. ~~4D~~[4D \(three spatial dimensions and one temporal dimension\)](#) reconstruction of
16 environmental dynamics. For instance, the concept of sediment connectivity (Bracken et al.,
17 2014) can be approached from a new perspective through varying ~~time and space~~[spatio-](#)
18 [temporal](#) scales. ~~Furthermore~~[Thereby](#), the magnitude and frequency of events and their
19 interaction can [also](#) be evaluated-~~from a novel point~~. ~~Furthermore, the versatility of view-~~
20 ~~Also, the possibility to reconstruct surfaces from~~ SfM photogrammetry utilising images,
21 captured from aerial or terrestrial perspectives, ~~inherits~~[has](#) the advantage ~~to be of being~~
22 applicable in [remote areas with limited access and in](#) fragile ~~and~~, fast changing environments.

23 After the suitability of SfM has been noticed for geo-scientific applications (James and
24 Robson, 2012, Westoby et al., 2012, Fonstad et al., 2013) the number of studies utilising SfM
25 photogrammetry [for geomorphometric investigations \(thereby referring to the “science of](#)
26 [topographic quantification” after Pike et al., 2008\)](#) has increased significantly. However, the
27 method needs sophisticated study design and some experience in image acquisition to prevent
28 predictable errors and to ensure good quality of the reconstructed scene. ~~James and Robson~~
29 ~~(2012)~~[Smith et al. \(2015\)](#) and Micheletti et al. (2015) recommend a setup for efficient data
30 acquisition.

31 A total of ~~61~~[65](#) publications are reviewed in this study. They are chosen according to the
32 respective field of research and methodology. Only studies are included that make use of the
33 benefits of automatic image matching algorithms and thus apply the various SfM tools.

1 Studies that lack of full automatisaton are excluded, i.e. some traditional photogrammetric
2 software. Topic wise a line is drawn in regard to the term geosciences. The largest fraction of
3 the reviewed articles tackles questions arising in geomorphological contexts. To account for
4 the versatility of SfM photogrammetry, a few studies deal with plant growth on different
5 scales (moss, crops, forest) or investigate rather exotic topics such as stalagmites or reef
6 morphology.

7 This review aims to highlight the development of SfM photogrammetry as a ~~promising~~great
8 tool for geoscientists:

9 (1) The method of SfM photogrammetry is briefly summarised and algorithmic differences
10 due to their emergence from computer vision as well as photogrammetry are clarified-
11 (section 2).

12 (2) Open-source tools regarding SfM photogrammetry are introduced as well as beneficial
13 tools for data post-processing (section 3).

14 ~~(2)~~(3) Different fields of applications where SfM photogrammetry led to new perceptions in
15 geomorphometry are displayed- (section 4).

16 ~~(3)~~(4) The performance of the reviewed method is evaluated- (section 5).

17 ~~(4)~~(5) And frontiers and significance of SfM photogrammetry are discussed- (section 6).

18

19 **2 SfM photogrammetry: ~~state-of-the-art~~method outline**

20 2.1 Basic concept

21 Reconstruction of three-dimensional geometries from images has played an important role in
22 the past centuries (Ducher, 1987, Collier, 2002). The production of high-resolution DEMs
23 was and still is one of the main applications of (digital) photogrammetry. Software and
24 hardware developments as well as the increase in computing power in the 1990s and early
25 2000s made aerial photogrammetric processing of large image datasets accessible to a wider
26 community (e.g. Chandler, 1999).

27 Camera orientations and positions, which are usually unknown during image acquisition, have
28 to be reconstructed to model a 3D scene. For that purpose, photogrammetry has developed
29 bundle ~~block~~-adjustment (BBABA) techniques, which allowed for simultaneous
30 determination of camera orientation and position parameters as well as 3D object point
31 coordinates for a large number of images- (e.g. Triggs et al, 2000). The input into the BBABA
32 are image coordinates of many tie points, ~~usually at least nine homologous points per image.~~
33 If the BBABA is extended by a simultaneous calibration option, even the intrinsic camera

1 parameters can be determined in addition to the extrinsic parameters. Furthermore, a series of
2 ground control points can be used as input into [BBABA](#) for geo-referencing the image block
3 (e.g. Luhmann et al., 2014, Kraus, 2007, Mikhail et al., 2001).

4 Parallel developments in computer vision took place that try to reconstruct viewing
5 geometries of image datasets not fulfilling the common prerequisites from digital
6 photogrammetry, i.e. calibrated cameras and initial estimates of the image acquisition scheme.
7 This led to the ~~structure from motion (SfM)~~ technique (Ullman, 1979) allowing to process
8 large datasets and to use a combination of multiple non-metric cameras.

9 The typical workflow of SfM photogrammetry (e.g. Snavely et al., 2008) comprises the
10 following steps (~~Fig. 1~~):

- 11 (1) identification and matching of homologous image points in overlapping photos (image
12 matching),
- 13 (2) reconstruction of the geometric image acquisition configuration and of the corresponding
14 3D coordinates of matched image points (sparse point cloud) with iterative [BBABA](#),
- 15 (3) dense matching of the sparse point cloud from reconstructed image network geometry.

16 ~~Image matching is fully automated in SfM tools, and different interest operators can be used
17 to select suitable image matching points. One of the most prominent examples for these
18 matching algorithms are both the “scale invariant feature transformation algorithm” (SIFT)
19 and the “Speeded up robust features algorithm” (SURF). In depth descriptions of SIFT and
20 SURF are given by Lowe (1999) and Bay (2008). These algorithms detect features (e.g.
21 Harris corners) that are robust to image scaling, image rotation, changes in perspective and
22 illumination. The detected features are localised in both the spatial and frequency domain and
23 are highly distinctive, which allows differentiating one feature from a large database of other
24 features (Lowe, 2004, Mikolajczyk, 2005). In contrast, kernel based correlation techniques are
25 normally used in photogrammetry, which are more precise (Grün, 2012), but more
26 constrained in regard to image configurations. When applied to oblique imagery, these kernel
27 based correlation techniques are outperformed by the new feature based algorithms especially
28 designed in order to match datasets from unstructured image acquisitions (Grün, 2012).~~

- 29 ~~(4) The information of the positions of the homologous image points is then used to
30 reconstruct the image network geometry, the 3D object point coordinates and the internal
31 camera geometry in an iterative BBA procedure (e.g. Pears et al., 2012). SfM
32 photogrammetry algorithms derive initial scene geometry by a comparatively large
33 number of common features found by the matching algorithms in one pair of images~~

1 ~~(Lowe, 2004). These extrinsic parameters are estimated usually using the “random~~
2 ~~sampling consensus” (RANSAC) algorithm (Fischler and Bolles, 1981), insensitive to~~
3 ~~relatively high number of false matches and outliers. This initial estimation of extrinsic~~
4 ~~parameters is refined in an iterative least-square minimization process, which also~~
5 ~~optimizes the cameras intrinsic parameters (camera self-calibration) for every single~~
6 ~~image. In contrast to classical photogrammetry software tools, SfM also scaling or geo-~~
7 ~~referencing, which is also performable within step 2.~~

8 Smith et al. (2015) give a detailed description of the workflow of SfM photogrammetry,
9 especially regarding step 1 and step 2.

10 In contrast to classical photogrammetry software tools, SfM allows for reliable processing of
11 a large number of images in rather irregular image acquisition schemes (Snavely et al., 2008)
12 and realises with a much higher degree of process automation. Thus, one of the main
13 differences between usual photogrammetric workflow and SfM is the emphasis on either
14 accuracy or automation, with SfM focusing on the latter (Pierrot-Deseilligny and Clery,
15 2011). Another deviation between both 3D reconstruction methods is the consideration of
16 GCPs (James and Robson, 2014, Eltner and Schneider, 2015). Photogrammetry performs
17 BBABA either one-staged, considering GCPs within the BBABA, or two-staged, performing
18 geo-referencing after a relative image network configuration has been estimated (Kraus,
19 2007). In contrast, SfM is solely performed in the manner of a two-staged BBABA
20 concentrating on the relative orientation in an arbitrary coordinate system. Thus, absolute
21 orientation has to be conducted separately with a seven parameter 3D-Helmert transformation,
22 i.e. three shifts, three rotations and one scale. This can be done, for instance, with the freeware
23 tool sfm-georef that also gives accuracy information (James and Robson, 2012). Using GCPs
24 has been proven to be relevant for specific geometric image network configurations, as
25 parallel-axes image orientations usual for UAV data, because adverse error propagation can
26 occur due to unfavourable parameter correlation, e.g. resulting in the non-linear error of a
27 DEM dome (Wu, 2014, James and Robson, 2014, Eltner and Schneider, 2015). Within a one-
28 staged BBABA these errors are avoided/minimised because during the adjustment calculation
29 additional information from GCPs is employed, which is not possible, when relative and
30 absolute orientation are not conducted in one stage.

31 The resulting oriented image block allows for a subsequent dense matching, measuring many
32 more surface points through spatial intersection to generate a DSM/DEM with very high
33 resolution. Recent developments in dense matching allow for resolving object coordinates for

1 almost every pixel. To estimate 3D coordinates, pixel values are either compared in image-
2 space in the case of stereo-matching, considering two images, or in the object space in the
3 case of MVS-matching, considering more than two images (Remondino et al., 2014).
4 Furthermore, local or global optimisation functions (Brown et al., 2003) are considered, e.g.
5 to handle ambiguities and occlusion effects between compared pixels (e.g. Pears et al., 2012).
6 To optimise ~~the pixel~~ matchmatching, (semi-)global constraints consider the entire image or
7 image scan-lines (~~usually utilised for stereo matching, Remondino et al., 2014;~~ e.g. semi-
8 global matching (SGM) after Hirschmüller, 2011), whereas local constraints consider a small
9 area in direct vicinity of the pixel of interest (~~usually utilised for MVS matching, Remondino~~
10 et al., 2014).

11 SfM photogrammetry software packages are available partially as freeware or even open-
12 source (~~e.g. Visual SfM, Bundler or APERO~~). Most of the packages comprise SfM
13 techniques in order to derive 3D reconstructions from any collection of unordered
14 photographs, without the need of providing camera calibration parameters and high accuracy
15 ground control points. As a consequence, no in-depth knowledge in photogrammetric image
16 processing is required in order to reconstruct geometries from overlapping image collections
17 (James and Robson, 2012, Westoby et al., 2012, Fonstad et al., 2013). But now, also many
18 photogrammetric tools utilise abilities from SfM to derive initial estimates automatically (i.e.
19 automation) and then perform photogrammetric BBABA with the possibility to set weights of
20 parameters for accurate reconstruction performance (i.e. accuracy). In this review studies are
21 considered, which either use straight SfM tools from computer vision or photogrammetric
22 tools implementing SfM algorithms that entail no need for initial estimates in any regard.

23

24 **Application of 2.2 Tools for SfM photogrammetry and data post processing**

25 SfM methodologies rely inherently on automated processing tools which can be provided by
26 different non-commercial or commercial software packages. Within the commercial approach
27 PhotoScan (Agisoft LLC, Russia), Pix4D (Pix4D SA, Switzerland) and MENCI APS
28 (MENCI Software, Italy) represent complete solutions for 3D photogrammetric processing
29 that have been used in several of the reviewed works.

30 Initiatives based on non-commercial software have played a significant role in the
31 development of SfM photogrammetry approaches, either 1) open-source, meaning the source
32 code is available with a license for modification and distribution; 2) freely-available, meaning
33 the tool is free to use but no source code is provided or 3) under free web service with no

1 [access to the code, intermediate results or possible secondary data usage \(Table 2\). The](#)
2 [pioneer works by Snavely et al. \(2006, 2008\) and Furukawa and Ponce \(2010\) as well as](#)
3 [Furukawa et al. \(2010\) provided the basis to implement one of the first open-source](#)
4 [workflows for free SfM photogrammetry combining Bundler and PMVS2/CMVS as in](#)
5 [SfMToolkit \(Astre, 2015\). By 2007, the MicMac project, which is open-source software](#)
6 [originally developed for aerial image matching, became available to the public and later](#)
7 [evolved to a comprehensive SfM photogrammetry pipeline with further tools such as APERO](#)
8 [\(Pierrot-Deseilligny and Clery, 2011\).](#)

9 [Further contributors put their efforts in offering freely-available solutions based on Graphical](#)
10 [User Interfaces \(GUI\) for SfM photogrammetry \(VisualSfM by Wu, 2013\) and geo-](#)
11 [referencing \(sfm_georef by James and Robson, 2012\). The need for editing large point-cloud](#)
12 [entities from 3D reconstruction led to the development of open-source specific tools such as](#)
13 [Meshlab \(Cignoni et al., 2008\) or CloudCompare \(Girardeau-Montaut, 2015\), also](#)
14 [implementing GUIs. Sf3M \(Castillo et al., 2015\) exploits VisualSfM and sfm_georef and](#)
15 [additional CloudCompare command-line capacities for image-based surface reconstruction](#)
16 [and subsequent point cloud editing within one GUI tool. Overall, non-commercial](#)
17 [applications have provided a wide range of SfM photogrammetry related solutions that are](#)
18 [constantly being improved on the basis of collaborative efforts. Commercial software](#)
19 [packages are not further displayed due to their usual lack of detailed information regarding](#)
20 [applied algorithms and their black box approach.](#)

21 [A variety of tools of SfM photogrammetry \(at least 10 different\) are used within the differing](#)
22 [studies of this review \(Fig. 3\). Agisoft PhotoScan is by far the most employed software,](#)
23 [which is probably due to its ease of use. However, this software is commercial and works](#)
24 [after the black box principle, which is in contrast to the second most popular tools Bundler in](#)
25 [combination with PMVS or CMVS. The tool APERO in combination with MicMac focuses](#)
26 [on accuracy instead of automation \(Pierrot-Deseilligny and Clery, 2011\), which is different to](#)
27 [the former two. The high degree of possible user-software interaction that can be very](#)
28 [advantageous to adopt the 3D reconstruction to each specific case study might also be its](#)
29 [drawback because further knowledge into the method is required. Only a few studies have](#)
30 [used the software in geo-scientific investigations \(Bretar, et al., 2013, Stumpf et al., 2014,](#)
31 [Ouédraogo et al., 2014, Stöcker et al., 2015, Eltner and Schneider, 2015\).](#)

3 Approaches to identify key developments of SfM photogrammetry

The vast recognition of SfM photogrammetry resulted in a large variety of its implementation leading to methodological developments, which have validity beyond its original application. Thus regarding geomorphometric investigations, studies considering field of applications as well as evaluations of the method performance induced key advances for SfM photogrammetry to establish as a standard tool in geosciences (Table 3). In the following, the approaches are introduced concerning the selection and retrieval of scientific papers utilising SfM photogrammetry and methods illustrated concerning integrated consideration of error performance of SfM photogrammetry in geo-scientific studies.

3.1 Selection of scientific papers exploiting SfM photogrammetry

A survey of 6465 scientific papers published between 2012 and 2015 revealed was conducted, covering a wide range of applications of SfM photogrammetry for in geo-scientific analysis (see Appendix A). The for a detailed list). Common scientific journals, academic databases and standard online searches have been used to search for corresponding publications. Although, it has to be noted that our approach does not guarantee full coverage of the published works using SfM photogrammetry in geosciences. Nevertheless, various disciplines, locations and approaches from all continents are contained in this review (Fig. 2). To put research hot spots in perspective it should be taken into account that the amount of publications in each discipline is not only dependent on the applicability of the method in that specific field of research. To a greater degree it is closely linked to the overall number of studies, which in the end can probably be broken down to the actual amount of researchers in that branch of science. Relative figures revealing the relation between SfM photogrammetry oriented studies to all studies of a given field of research would be desirable but are beyond the scope of this review.

3.2 Performing error evaluation from recent studies

SfM photogrammetry has been tested under a large variety of environments due to the commensurate novel establishment of the method in geosciences, revealing numerous advantages but also disadvantages regarding to each application. It is important to have method independent references to evaluate 3D reconstruction tools confidently. In total 39 studies are investigated (Table Appendix A), where a reference has been setup, either area

1 based (e.g. TLS) or point based (e.g. RTK GPS points). Because not all studies perform
2 accuracy assessment with independent references, the number of studies is in contrast to the
3 number of 65 studies that are reviewed in regard to applications.

4 A designation of error parameters is performed prior to comparing the studies to avoid using
5 ambiguous terms. There is a difference between local surface quality and more systematic
6 errors, i.e. due to referencing and project geometry (James and Robson, 2012). Specifically,
7 error can be assessed in regard to accuracy and precision.

8 Measurement accuracy, which defines the closeness of the measurement to a reference ideally
9 displays the true surface and can be estimated by the mean error value. However, positive and
10 negative deviations can compensate for each other and thus can impede the recognition of a
11 systematic error (e.g. symmetric tilting) with the mean value. Therefore, numerical and spatial
12 error distribution should also be considered to investigate the quality of the measurement (e.g.
13 Smith et al., 2015). For the evaluation of two DEMs, the iterative closest point (ICP)
14 algorithm can improve the accuracy significantly if a systematic linear error (e.g. shifts, tilts
15 or scale variations) is given, as demonstrated by Micheletti et al. (2014); Nevertheless, this
16 procedure can also induce an error when the scene has changed significantly between the two
17 datasets.

18 Precision, which defines the repeatability of the measurement, e.g. it indicates how rough an
19 actual planar surface is represented, usually comprises random errors that can be measured
20 with the standard deviation or RMSE. However, precision is not independent from systematic
21 errors. In this study, the focus lies on RMSE or standard deviation calculated to a given
22 reference (e.g. to a LiDAR point cloud) and thus the general term “measured error” is used.

23 Furthermore, error ratios are calculated to compare SfM photogrammetry performance
24 between different studies under varying data acquisition and processing conditions. Thereby,
25 the relative error (e_r), the reference superiority (e_s) and the theoretical error ratio (e_t) are
26 considered. The first is defined as the ratio between measured error and surface to camera
27 distance (eq. 1).

$$28 \quad e_r = \frac{\sigma_m}{D} \quad \text{-----} \quad (1)$$

29 Being:

e_r ... relative error

σ_m ... measured error

D ... mean distance camera – surface

1
2 The reference superiority displays the ratio between the measured error and the error of the
3 reference (eq. 2). It depicts the validity of the reference to be accountable as a reliable dataset
4 for comparison.

$$5 \quad e_s = \frac{\sigma_m}{\sigma_{ref}} \quad \text{-----} \quad (2)$$

6 Being:

e_r ...reference superiority

σ_{ref} ...reference error

7
8 The theoretical error ratio includes the theoretical error, which is an estimate of the
9 theoretically best achievable photogrammetric performance under ideal conditions. It is
10 calculated separately for convergent and parallel-axes image acquisition schemes. The
11 estimate of the theoretical error of depth measurement for the parallel-axis case is displayed
12 by eq. 3 (more detail in Kraus, 2007). The error is determined for a stereo-image pair and thus
13 might overestimate the error for multi-view reconstruction. Basically, the error is influenced
14 by the focal length, the camera to surface distance and the distance between the images of the
15 stereo-pair (base).

$$16 \quad \sigma_p = \frac{D^2}{Bc} \sigma_i \quad \text{-----} \quad (3)$$

17 Being:

σ_p ...coordinate error for parallel – axes case

c ...focal length

σ_i ...error image measurement

18 *B... distance between images (base)*

19
20 For the convergent case the error also considers the camera to surface distance and the focal
21 length. However, instead of the base the strength of image configuration determined by the
22 angle between intersecting homologous rays is integrated and additionally the employed
23 number of images is accounted for (eq. 4; more detail in Luhmann et al., 2014).

$$24 \quad \sigma_c = \frac{qD}{\sqrt{kc}} \sigma_i \quad \text{-----} \quad (4)$$

1 Being:

σ_c ... coordinate error for convergent case

q ... strength of image configuration, i.e. convergence

k ... number of images

2
3 Finally, the theoretical error ratio is calculated displaying the relation between the measured
4 error and the theoretical error (eq. 5). The value depicts the performance of SfM
5 photogrammetry in regard to the expected accuracy.

$$6 \quad e_t = \frac{\sigma_m}{\sigma_{theo}} \quad \text{-----} \quad (5)$$

7 Being:

8 e_t ... theoretical error ratio

σ_{theo} ... theoretical error; either σ_p or σ_c

9
10 The statistical analysis of the achieved precisions of the reviewed studies is performed with
11 the Python Data Analysis Library (pandas). If several errors are given in one study due testing
12 of different survey or processing conditions, the error value representing the enhancement of
13 the SfM performance has been chosen, i.e. in the study of Javernick et al. (2014) the DEM
14 without an error dome, of Rippin et al. (2015) the linear corrected DEM, and of Eltner &
15 Schneider (2015) the DEMs calculated with undistorted images. In addition, if several
16 approaches are conducted to retrieve the deviations value to the reference, the more reliable
17 error measure is preferred (regards Stumpf et al., 2014 and Gómez-Gutiérrez et al., 2014 and
18 2015). Apart from those considerations, measured errors have been averaged if several values
19 are reported in one study, i.e. concerning multi-temporal assessments or consideration of
20 multiple surfaces with similar characteristics, but not for the case of different tested SfM
21 tools. Regarding data visualisation, outliers that complicated plot drawing, were neglected
22 within the concerning graphics. This concerned the study of Dietrich (2016) due to a very
23 large scale of an investigated river reach (excluded from Fig. 4a and Fig. 5a-b), the study of
24 Snapir et al. (2014) due to a very high reference accuracy of Lego bricks (excluded from Fig.
25 4c and Fig. 5b), and Frankl et al. (2015) due to a high measured error as the study focus was
26 rather on feasibility than accuracy (excluded from Fig. 5c).

27 Besides exploiting a reference to estimate the performance of the 3D reconstruction,
28 registration residuals of GCPs resulting from BA can be taken into account for a first error
29 assessment. But it is not suitable as exclusive error measure due to potential deviations

1 between the true surface and the calculated statistical and geometric model, which are not
2 detectable with the GCP error vectors alone because BA is optimised to minimise the error at
3 these positions. However, if BA has been performed two-staged (i.e. SfM and referencing
4 calculated separately), the residual vector provides reliable quality information because
5 registration points are not integrated into model estimation.

6

7 **4 Recent applications of SfM photogrammetry in geosciences**

8 The previously described advantages of the method ~~introduce~~has introduced a new group of
9 users, leading to a variety of new studies in geomorphic surface reconstruction and analysis.
10 Different disciplines started to use SfM algorithms more or less simultaneously. ~~It should be~~
11 ~~noted that common scientific journals, databases and standard online searches do not~~
12 ~~guarantee complete coverage of all studies about SfM photogrammetry in geosciences.~~
13 ~~Nevertheless, various disciplines, locations and approaches from all continents are contained~~
14 ~~in this review (Fig. 2).~~

15 A list of all topics reviewed in this manuscript according to their year of appearance is shown
16 in Table 24. It is important to note that most subjects are not strictly separable from each
17 other: For instance, a heavy flash flood event will likely trigger heavy damage by soil erosion
18 or upstream slope failures. Thus, corresponding studies are arranged in regard to their major
19 focus. The topic soil science comprises studies of soil erosion as well as soil micro-
20 topography.

21 ~~To put research hot-spots in perspective it should be taken into account, that the number of~~
22 ~~publications from each discipline is not only dependent on the applicability of the method in~~
23 ~~that specific field of research. To a greater degree it is closely linked to the overall number of~~
24 ~~studies, which in the end can probably be broken down to the actual amount of researchers in~~
25 ~~that branch of science. Relative figures revealing the relation between SfM photogrammetry~~
26 ~~oriented studies to all studies of a given field of research would be desirable but are beyond~~
27 ~~the scope of this review.~~

28 3

29 **4.1 Soil science**

30 An identification of convergent research topics of SfM photogrammetry in geosciences
31 revealed a distinct focus on erosional processes, especially in soil erosion (11 studies).
32 Gullies, as often unvegetated and morphologically complex features of soil erosion, are

1 | predestined to serve as a research object (6 studies) to evaluate SfM [photogrammetry](#)
2 | performance. One of the first works on SfM in geosciences from 2012 compared established
3 | 2D and 3D field methods for assessing gully erosion (e.g. [light detection and ranging -](#)
4 | [LiDAR](#), profile meter, total station) to SfM ~~[photogrammetry with data with](#)~~ regard to costs,
5 | accuracy and effectiveness revealing the superiority of ~~[SfM photogrammetry the method](#)~~
6 | (Castillo et al., 2012). Also for a gully system, Stöcker et al. (2015) demonstrated the
7 | flexibility of ~~[SfM photogrammetry by camera based surface reconstruction by](#)~~ combining
8 | independently captured terrestrial images with ~~[reconstructed](#)~~ surface models from UAV
9 | images to fill data gaps and achieve a comprehensive 3D model. ~~[Another advantage of SfM](#)~~
10 | ~~[photogrammetry - surface measurement of large](#)~~ [Large areal](#) coverage ~~[with and](#)~~ very high
11 | resolution - allowed for a new [quality in the](#) assessment of plot based soil erosion analysis
12 | (Eltner et al., 2015)

13 | Another 6 studies tackle the 3D reconstruction of soil micro-topography by producing very
14 | dense point clouds or DEMs. This data further serves to assess pros and cons of SfM
15 | photogrammetry, e.g. ~~[with regard to the doming effect \(Eltner and Schneider, 2015\)](#)~~, to detect
16 | small-scale erosion features (Nouwakpo et al., 2014), [with regard to the doming effect \(Eltner](#)
17 | [and Schneider, 2015\)](#) or as input parameter for erosion modelling (Kaiser et al., 2015).

18 | **[34.2](#) Volcanology**

19 | Volcanology is a pioneering area of SfM photogrammetry research in geosciences because 3
20 | out of 6 studies in 2012 included volcanic research sites. James and Robson (2012) acquired
21 | information on volcanic dome volume and structural variability prior to an explosion from
22 | multi-temporal imagery taken from a light airplane. ~~[Brotheland et al. \(2015\) also surveyed](#)~~
23 | ~~[volcanic dome dynamics with airborne imagery, but at larger scale for a resurgent dome.](#)~~
24 | Another interesting work by Bretar et al. (2013) successfully reveals roughness differences in
25 | volcanic surfaces from lapilli deposits to slabby pahoehoe lava.

26 | **[34.3](#) Glaciology**

27 | Glaciology and associated moraines are examined in 7 publications. ~~[Rippin et al. \(2015\)](#)~~
28 | ~~[present a fascinating UAV-based work on supra-glacial runoff networks, comparing the](#)~~
29 | ~~[drainage system to surface roughness and surface reflectance measurements and detecting](#)~~
30 | ~~[linkages between all three.](#)~~ In several UAV campaigns Immerzeel et al. (2014) detected
31 | limited mass losses and low surface velocities but high local variations of melt rates that are
32 | linked to supra-glacial ponds and ice cliffs. [Rippin et al. \(2015\) present another UAV-based](#)
33 | [work on supra-glacial runoff networks, comparing the drainage system to surface roughness](#)

1 [and surface reflectance measurements and detecting linkages between all three. Furthermore,](#)
2 [snow depth estimation and rock glacier monitoring are increasingly performed with SfM](#)
3 [photogrammetry \(Nolan et al., 2015, Dall'Asta et al., 2015\).](#)

4 **34.4 Mass movements**

5 [Compared to the well-established use of LiDAR techniques on the investigation of landslides](#)
6 [\(Jaboyedoff et al., 2012\) the use of photogrammetric workflows for investigating hazardous](#)
7 [slopes is still scarce, which is probably due to the stringent accuracy and safety](#)
8 [requirements. For instance, the use of UAV systems for monitoring mass movements using](#)
9 [both image correlation algorithms and DM subtraction techniques has been explored by](#)
10 [Lucieer et al., \(2013\). More recently, SfM techniques were ~~monitored~~ used by Stumpf et al.](#)
11 [\(2014\) ~~at a~~ for monitoring landslide displacements and erosion during several measuring](#)
12 [campaigns, including the study of seasonal dynamics on the landslide body, superficial](#)
13 [deformation and rock fall occurrence. In addition, these authors assessed the accuracy of two](#)
14 [different 3D reconstruction tools ~~were tested and~~ compared to LiDAR data. ~~Furthermore,~~](#)
15 [~~seasonal dynamics of the landslide body and different processes, like lobes and rock fall,~~](#)
16 [~~could be separated.~~](#)

17 **34.5 Fluvial morphology**

18 Channel networks in floodplains were surveyed by Prosdocimi et al. (2015) in order to
19 analyse eroded ~~channels~~ channel banks and to quantify the transported material. Besides
20 classic DSLR cameras, evaluation of an iPhone camera revealed sufficient accuracy, so that in
21 near future also ~~farmers~~ non-scientist are able to carry out post event documentation of
22 damage. An interesting large scale riverscape assessment is presented by Dietrich (2016), who
23 carried out a helicopter based data acquisition of a 32 km river segment. A small helicopter
24 proves to close the gap between unmanned platforms and commercial aerial photography
25 from airplanes.

26 **34.6 Coastal morphology**

27 In the ~~pioneering~~ article by Westoby et al. (2012) several morphological features of
28 contrasting landscapes were chosen to test the capabilities of SfM; one of them being a
29 coastal cliff of roughly 80 m height. Up to 90.000 points/m² enabled the identification of
30 bedrock faulting. Ružić et al. (2014) produced surface models of coastal cliffs ~~that have been~~
31 ~~retreating up to 5 m since the 1960s~~ to test the abilities of SfM photogrammetry in undercuts
32 and complex morphologies.

3.7—Others

4.7 Other fields of investigation in geosciences

In addition to the prevalent fields of attention also more exotic research is carried out unveiling unexpected possibilities for SfM photogrammetry. Besides the benefit for the specific research itself, these branches are important as they either explore new frontiers in geomorphometry or demonstrate the versatility of the method. Lucieer et al. (2014) analyse arctic moss beds and their health conditions by using high-resolution surface topography (2 cm DEM) to simulate water availability from snow melt. Leon et al. (2015) acquired underwater imagery of a coral reef to produce a DEM with a resolution of 1 mm for roughness estimation. Genchi et al. (2015) used UAV-image data of an urban cliff structure to identify bio erosion features and found a pattern in preferential locations.

The re-consideration of historical aerial images is another interesting opportunity arising from the new algorithmic image matching developments that allow for new DEM resolutions and thus possible new insights into landscape evolution (Gomez et al., 2015). ~~Also accounting for the temporal scale, completely new insights can be achieved by time lapse analysis, already demonstrated by James and Robson (2014b), who monitored a lava flow at minute intervals.~~

3—Non-commercial tools for SfM photogrammetry and data post-processing

~~Initiatives based on non-commercial software have played a significant role in the development of SfM photogrammetry approaches, either open-source, meaning the source code is available with a license for modification and distribution, or freely available, meaning the tool is free to use but no source code is provided (Appendix B). The pioneer works by Snavely et al. (2006, 2008) and Furukawa and Ponce (2010) as well as Furukawa et al. (2010) provided the basis to implement one of the first open-source workflows for free SfM photogrammetry combining Bundler and PMVS2/CMVS as in SfMToolkit (Astre, 2015). By 2007, the MicMac project, which is open-source software originally developed for aerial image matching, became available to the public and later evolved to a comprehensive SfM photogrammetry pipeline with further tools such as APERO (Pierrot-Deseilligny and Clery, 2011).~~

~~Further contributors put their efforts in offering freely available solutions based on Graphical User Interfaces (GUI) for image-based 3D reconstruction (VisualSfM by Wu, 2013) and geo-referencing (sfm_georef by James and Robson, 2012). The need for editing large point cloud~~

1 entities from 3D reconstruction led to the development of open-source specific tools such as
2 Meshlab (Cignoni et al., 2008) or CloudCompare (Girardeau-Montaut, 2015), also
3 implementing GUIs. Sf3M (Castillo et al., 2015) exploits VisualSfM and sfm_georef and
4 additional CloudCompare command-line capacities for image-based surface reconstruction
5 and subsequent point cloud editing within one GUI tool. Overall, non-commercial
6 applications have provided to date a wide range of SfM photogrammetry related solutions that
7 are constantly being improved on the basis of collaborative efforts.

8 A variety of tools of SfM photogrammetry (at least 10 different) are used within the differing
9 studies of this review (Fig. 3). Agisoft PhotoScan is by far the most employed software,
10 which is probably due to its ease of use. However, this software is commercial and works
11 after the black box principle, which is in contrast to the second most popular tools Bundler in
12 combination with PMVS or CMVS. The tool APERO in combination with MicMac focuses
13 on accuracy instead of automation (Pierrot-Deseilligny and Clery, 2011), which is different to
14 the former two. The high degree of possible user software interaction that can be very
15 advantageous to adopt the 3D reconstruction to each specific case study might also be its
16 drawback because further knowledge into the method is required. Only a few studies have
17 used the software in geo-scientific investigations (Bretar, et al., 2013, Stumpf et al., 2014,
18 Ouédraogo et al., 2014, Stöcker et al., 2015, Eltner and Schneider, 2015).

20 **4— Performance of SfM photogrammetry in geo-scientific applications**

21 It is important to have method-independent references to evaluate 3D reconstruction tools
22 confidently. This time, 39 studies are investigated (Table Appendix A), where a reference has
23 been setup, either area based (e.g. TLS) or point based (e.g. RTK-GPS points). Because not all
24 studies perform accuracy assessment with independent references, the number of studies is in
25 contrast to the number of 61 studies that were reviewed in regard to applications in Sect. 3.

26 **5.1— Error terms**

27 A definite designation of error parameters is performed prior to comparing the studies to
28 avoid using ambiguous terms. There is a difference between local surface quality and more
29 systematic errors, i.e. due to referencing and project geometry (James and Robson, 2012).
30 Specifically, error can be assessed in regard to accuracy and precision.

31 Accuracy defines the closeness of the measurement to the true surface and usually implies
32 systematic errors, which can be displayed by the mean error value. For the evaluation of two

1 ~~DEMs, the iterative closest point (ICP) algorithm can improve the accuracy significantly if a~~
2 ~~systematic linear error (e.g. shifts, tilts or scale variations) is given, as demonstrated by~~
3 ~~Micheletti et al. (2014).~~

4 ~~Precision defines the repeatability of the measurement, e.g. it indicates how rough an actual~~
5 ~~planar surface is represented. Precision usually comprises random errors and is measured with~~
6 ~~the standard deviation or RMSE. However, precision is not independent from systematic~~
7 ~~errors. In this study, focus lies on precision which also might be influenced by systematic~~
8 ~~errors and thus the general term “measured error” is used.~~

9 ~~Registration residuals of GCPs resulting from BBA allow for a first error assessment. But it is~~
10 ~~not sufficient as exclusive error measure due to potential deviations between the true surface~~
11 ~~and the calculated statistical and geometric model, which are not detectable with the GCP~~
12 ~~error vectors alone because BBA is optimised to minimise the error at these positions.~~
13 ~~However, if BBA has been performed two-staged (i.e. SfM and referencing calculated~~
14 ~~separately), the residual vector provides reliable quality information because registration~~
15 ~~points are not integrated into model estimation.~~

16 ~~Further~~

17 **5 Error assessment of SfM photogrammetry in geo-scientific applications**

18 Error evaluation in this study is performed with reference measurements. Thereby, errors due
19 the performance of the method itself and errors due to the method of quality assessment have
20 to be distinguished.

21 **5.21 Error sources of image-based 3D reconstruction****SfM photogrammetry**

22 The error of 3D reconstruction is influenced by many factors: scale/distance, camera
23 calibration, image network geometry, image matching performance, surface texture and
24 lighting conditions, and GCP characteristics, which are examined in detail in this section. ~~The~~
25 ~~statistical analysis of the achieved accuracies of the reviewed studies is performed with the~~
26 ~~Python Data Analysis Library (panda). If several errors were measured with the same setup,~~
27 ~~e.g. in the case of multi-temporal assessments, the average value is applied. Furthermore,~~
28 ~~outliers that complicated data visualisation, were neglected within the concerning plots. This~~
29 ~~concerned the study of Dietrich (2016) due to a large scale, the study of Snapir et al. (2014)~~
30 ~~due to a high reference accuracy and Frankl et al. (2015) due to a high measured error.~~

31 *Scale and sensor to surface distance*

1 SfM photogrammetry contains the advantage to be useable at almost any scale. Thus, in the
2 reviewed studies the method is applied at a large range of scales (Fig. 4 [a](#)), reaching from
3 10 cm for volcanic bombs (Favalli et al., 2012, James and Robson, 2012) up to 10 km for a
4 river reach (Dietrich, 2016). Median scale amounts about 100 m. SfM photogrammetry
5 reveals a scale dependent practicability (Smith and Vericat, 2015) if case study specific
6 tolerable errors are considered, e.g. for multi-temporal assessments. For instance, at plot and
7 hillslope scale 3D reconstruction is a very sufficient method for soil erosion studies, even
8 outperforming TLS (Nouwakpo et al., 2015, Eltner et al., 2015, Smith and Vericat, 2015). The
9 method should be most useful in small scale study reaches (Fonstad et al., 2013), whereas
10 error behaviour is not as advantageous for larger scales, i.e. catchments (Smith and Vericat,
11 2015).

12 Besides scale, ~~observation of~~ the distance between sensor and surface is important for image-
13 based reconstructed DEM error, also because scale and distance interrelate. The comparison
14 of the reviewed studies indicates that with an increase of distance the measured error
15 decreases, which is not unexpected (Fig. 5 [a](#), circles). However, there is no linear trend
16 detectable. Therefore, ~~a uniform error ratio (or the relative error), which is calculated by~~
17 ~~dividing distance with measured error,~~ is not assignable. The [relative](#) error ~~ratio itself~~ displays
18 a large range from 15 to 4000 with a median of 400, thus revealing a rather low error potential
19 (Fig. 5 [a](#), triangles). Very high ratios are solely observable for very close-range applications
20 and at large distances. A general increase of the [relative](#) error ~~ratio~~ with distance is observable
21 (Fig. 5 [a](#), triangles). The indication that cm-accurate measurements are realisable at distances
22 below 200 m (Stumpf et al., 2014) can be confirmed by Fig. 5 [a](#) because most deviations are
23 below 10 cm until that range. Overall, absolute error values are low at close ranges, whereas
24 the [relative](#) error ~~ratio~~ is higher at larger distances.

25 *Camera calibration*

26 SfM photogrammetry allows for straight forward handling of camera options due to integrated
27 self-calibration, but knowledge about some basic parameters is necessary to avoid unwanted
28 error propagation into the final DEM from insufficiently estimated camera models. The
29 autofocus as well as automatic camera stabilisation options should be deactivated if a pre-
30 calibrated camera model is used or one camera model is estimated for the entire image block
31 because changes in the interior camera geometry due to camera movement cannot be captured
32 with these settings. The estimation of a single camera model for one image block is usually
33 preferable, if a single camera has been used, whose interior geometry is temporary stable, to

1 avoid over parameterisation (Pierrot-Deseilligny and Clery, 2011). Thus, if zoom lenses are
2 moved a lot during data acquisition, they should be avoided due to their instable geometry
3 (Shortis et al., 2006, Sanz-Ablanedo et al., 2010) that impedes usage of pre-calibrated fixed or
4 single camera models. A good compromise between camera stability, sensor size and
5 equipment weight, which is more relevant for UAV applications, are achieved by compact
6 system cameras (Eltner and Schneider, 2015). However, solely three studies utilize compact
7 system cameras in the reviewed studies (Tonkin et al., 2014, Eltner and Schneider, 2015,
8 Eltner et al., 2015).

9 Along with camera settings, the complexity in regard to the considered parameters of the
10 defined camera model within the 3D reconstruction tool is relevant, ~~i.e. as well as the~~
11 ~~implementation of GCPs to function as further observation in the BA, i.e. to avoid DEM~~
12 ~~domes as a consequence of insufficient image distortion estimation (James and Robson, 2014,~~
13 ~~Eltner and Schneider, 2015). Also, Stumpf et al. (2014) detect worse distortion correction~~
14 ~~with a basic SfM tool, considering a simple camera model, compared to more complex~~
15 ~~software, integrating a variety of camera models-~~ and GCP consideration. Camera calibration
16 is a key element for high DEM quality, which is extensively considered in photogrammetric
17 software, whereas simpler models that solely estimate principle distance and radial distortion
18 are usually implemented in the SfM tools originating from computer vision (Eltner and
19 Schneider, 2015, James and Robson, 2012, Pierrot-Deseilligny and Clery, 2011). ~~Fig. 6 also~~
20 ~~demonstrates that at same distances more extensive 3D reconstruction tools, implementing~~
21 ~~more complex camera models and several GCP integration possibilities (e.g. APERO, Pix4D,~~
22 ~~Agisoft PhotoScan) produce lower errors compared to tools considering basic camera models~~
23 ~~and no GCPs (e.g. Visual SfM, Bundler).~~

24 *Image resolution*

25 Image resolution is another factor influencing the final DEM quality. Especially, the absolute
26 pixel size needs to be accounted for due to its relevance for the signal-to-noise ratio (SNR)
27 because the larger the pixel the higher the amount of light that can be captured and hence a
28 more distinct signal is measured. Resolution alone by means of pixel number gives no
29 information about the actual metric sensor size. A large sensor with large pixels and a large
30 amount of pixels provides better image quality due to reduced image noise than a small sensor
31 with small pixels but the same amount of pixels. Thus, high image resolution defined by large
32 pixel numbers and pixel sizes resolves in sufficient quality of images and thus DEMs
33 (Micheletti et al., 2014, Eltner and Schneider, 2015).

1 However, ~~in this study~~ the reviewed investigations indicate no obvious influence of the pixel
2 size at the DEM quality ~~(Fig. 7)~~. Mostly, cameras with middle sized sensors and
3 corresponding pixel sizes around 5 μm are used. ~~In studies with pixel sizes larger 7 μm an~~
4 ~~error ratio above 500 is observable. But else and~~ a large range of error at different pixel sizes
5 ~~can be seen, which might be due to other error influences superimposing the impact of pixel~~
6 ~~size. Thus, more data is needed for significant conclusions is given.~~

7 To speed up processing, down-sampling of images is often performed causing interpolation of
8 pixels and thus the reduction of image information, which can be the cause for
9 underestimation of high relief changes, e.g., observed by Smith and Vericat (2015) or
10 Nouwakpo et al. (2015). Interestingly, Prosdocimi et al. (2015) reveal that lower errors are
11 possible with decreasing resolution due to an increase of error smoothing. Nevertheless,
12 image data collection in the field should be done at highest realisable resolution and highest
13 SNR to fully keep control over subsequent data processing, i.e. data smoothing should be
14 performed under self-determined conditions at the desktop, which is especially important for
15 studies of rough surfaces to allow for probate error statistics (e.g. Brasington et al., 2012).

16 *Image network geometry*

17 In regard to the geometry of the image network several parameters are important: number of
18 images, image overlap, obliqueness, and convergence.

19 At least three images need to capture the area of interest, but for redundancy to decrease DEM
20 error higher numbers are preferred (James and Robson, 2012). For instance, Piermattei et al.
21 (2015) detect better qualities for a higher amount of images. However, the increase of images
22 does not linearly increase the accuracy (Micheletti et al., 2014), and may ultimately lead to
23 unnecessary increase in computation time. Generally, image number should be chosen
24 depending on the size and complexity of the study reach (James and Robson, 2012); as high
25 as possible but still keeping in mind acceptable processing time. ~~The reviewed studies do not~~
26 ~~allow for distinct relation conclusions between 3D reconstruction performance and image~~
27 ~~number because the DEM error also interferes with other parameters, e.g. such as object~~
28 ~~complexity, image overlap or image convergence (Fig. 8).~~

29 High image overlap is relevant to finding homologous points within many images that cover
30 the entire image space. Stumpf et al. (2014) show that higher overlap resolves in better
31 results, ~~even though ground sampling distance decreases due to a smaller focal length.~~ Wide
32 angle lenses, whose radial distortion is within the limits, should be chosen for data
33 acquisition.

1 The reviewed studies reveal a large variety of applicable perspectives for DEM generation
2 ([Table 3](#)). Most applications use images captured from the ground, which is the most flexible
3 implementation of the SfM photogrammetry method. In regard to terrestrial or aerial
4 perspective, Smith and Vericat (2015) state that aerial images should be preferred if plots
5 reach sizes larger 100 m because at these distances obliqueness of images becomes too
6 adverse. Stumpf et al. (2014) even mention a distinct value of the incidence angle of 30° to
7 the captured surface above which data quality decreases significantly.

8 Furthermore, image network geometry has to be considered separately for convergent
9 acquisitions schemes, common for terrestrial data collection, and for parallel-axes acquisition
10 schemes, common for aerial data collection. The parallel-axes image configuration results in
11 unfavourable error propagation due to unfavourable parameter correlation, which inherits the
12 separation between DEM shape and radial distortion (James and Robson, 2014, Wu, 2014)
13 resulting in a dome error that needs either GCP implementation or a well estimated camera
14 model for error mitigation (James and Robson, 2014, Eltner and Schneider, 2015). However,
15 GCP accuracy has to be sufficient or else the weight of GCP information during [BBABA](#) is
16 too low to avoid unfavourable correlations, as shown by Dietrich (2016), where DEM dome
17 error within a river reach could not be diminished even though GCPs were implemented into
18 3D reconstruction. If convergent images are utilised, the angle of convergence is important
19 because the higher the angle the better the [image network geometry](#) ~~and thus~~. [Thereby,](#)
20 accuracy [increases](#) because sufficient image overlap [is possible](#) with larger bases between
21 images ~~is possible and thus less difficulties due to~~. [Therefore,](#) glancing ray intersections ~~arise,~~
22 [which impede distinct depth assignment, are avoided](#). But simultaneously, convergence
23 should not be so high that the imaged scene becomes too contradictory for successful image
24 matching (Pierrot-Deseilligny and Clery, 2012, Stöcker et al, 2015).

25 *Accuracy and distribution of homologues image points*

26 The quality of DEMs reconstructed from overlapping images depends significantly on the
27 image-matching performance (Grün, 2012). Image content and type, which cannot be
28 enhanced substantially, are the primary factors controlling the success of image-matching
29 (Grün, 2012). Image-matching is important for reconstruction of the image network geometry
30 as well as the subsequent dense-matching.

31 On the one hand, it is relevant to find good initial matches (e.g. SIFT features are not as
32 precise as least square matches with $\frac{1}{10}$ pixel size accuracies; Grün, 2012) to perform reliable
33 3D reconstruction and thus retrieve an accurate sparse point cloud because [MVS approaches](#)

1 | ~~for dense matching as well as~~ optimization procedures for model refinement rely on this first
2 point cloud. Thus, immanent errors will propagate along the different stages of SfM
3 photogrammetry.

4 On the other hand, more obviously image-matching performance is important for dense
5 reconstruction, when 3D information is calculated for almost every pixel. The accuracy of
6 intersection during dense matching depends on the accuracy of the estimated camera
7 orientations (Remondino et al., 2014). If the quality of the DEM is the primary focus, which is
8 usually not the case for SfM algorithms originating from computer vision, the task of image-
9 matching is still difficult (Grün, 2012). Nevertheless, newer approaches are emerging, though,
10 which still need evaluation in respect of accuracy and reliability (Remondino et al., 2014). An
11 internal quality control for image-matching is important for DEM assessment (Grün, 2012),
12 | but are mostly absent in tools for ~~image-based 3D reconstruction~~[SfM photogrammetry](#).

13 So far, many studies exist, which evaluate the quality of 3D reconstruction in geo-scientific
14 applications. Nevertheless, considerations of dense-matching performance are still missing,
15 especially in regard of rough topographies (Eltner and Schneider, 2015).

16 *Surface texture*

17 Texture and contrast of the area of interest is significant to identify suitable homologues
18 image points. Low textured and contrasted surfaces result in a distinct decrease of image
19 features, i.e. snow covered glaciers (Gómez-Gutiérrez et al., 2014) or sandy beaches (Mancini
20 et al., 2013). Furthermore, vegetation cover complicates image matching performance due to
21 its highly variable appearance from differing viewing angles (e.g. Castillo et al., 2012, Eltner
22 | et al., 2015) and possible movements during wind. Thus, in this study, ~~if possible~~[where](#)
23 [present](#), only studies of bare surfaces are reviewed for error assessment.

24 *Illumination condition*

25 Over- and under-exposure of images is another cause of error in the reconstructed point cloud,
26 which cannot be significantly improved by utilising HDR images (Gómez-Gutiérrez et al.,
27 2015). Well illuminated surfaces result in a high number of detected image features, which is
28 demonstrated for coastal boulders under varying light conditions by Gienko and Terry (2014).
29 Furthermore, Gómez-Gutiérrez et al. (2014) highlight the unfavourable influence of shadows
30 because highest errors are measured in these regions; interestingly, these authors calculate the
31 optimal time for image acquisition from the first DEM for multi-temporal data acquisition.
32 | [Furthermore, the temporal length of image acquisition needs to be considered during sunny](#)

1 [conditions because with increasing duration shadow changes can decrease matching](#)
2 [performance, i.e. with regard to the intended quality surveys lasting more than 30 minutes](#)
3 [should be avoided \(Bemis et al., 2014\).](#) Generally, overcast but bright days are most suitable
4 for image capture to avoid strong shadows or glared surfaces (James and Robson, 2012).

5 *GCP accuracy and distribution*

6 GCPs are important inputs for data referencing and scaling. Photogrammetry always stresses
7 the weight of good ground control for accurate DEM calculation, especially if one-staged
8 [BBABA](#) is performed. In the common SfM workflow integration of GCPs is less demanding
9 because they are only needed to transform the 3D-model from the arbitrary coordinate system,
10 which is comparable to the photogrammetric two-staged [BBABA](#) processing. A minimum of
11 three GCPs are necessary to account for model rotation, translation and scale. However, GCP
12 redundancy, thus more points, has been shown to be preferable to increase accuracy (James
13 and Robson, 2012). A high number of GCPs further ensures the consideration of checkpoints
14 not included for the referencing, which are used as independent quality measure of the final
15 DEM. More complex 3D reconstruction tools either expand the original 3D-Helmert-
16 transformation by secondary refinement of the estimated interior and exterior camera
17 geometry to account for non-linear errors (e.g. Agisoft PhotoScan) or integrate the ground
18 control into the [BBA \(e.g. APERO\)-BA \(e.g. APERO\)](#). For instance, [Javernick et al. \(2014\)](#)
19 [could reduce the height error to decimetre level by including GCPs in the model refinement.](#)

20 Natural features over stable areas, which are explicitly identifiable, are an alternative for GCP
21 distributions, although they usually lack strong contrast (as opposed to artificial GCPs) that
22 would allow for automatic identification and sub-pixel accurate measurement (e.g. Eltner et
23 al., 2013). Nevertheless, they can be suitable for multi-temporal change detection
24 applications, where installation of artificial GCPs might not be possible [\(e.g. glacier surface](#)
25 [reconstruction; Piermattei et al., 2015\)](#) or necessary as in some cases relative accuracy is
26 preferred over absolute performance (e.g. observation of landslide movements, Turner et al.,
27 2015).

28 GCP distribution needs to be even and adapted to the terrain resulting in more GCPs in areas
29 with large changes in relief (Harwin and Lucieer, 2012) to cover different terrain types.
30 Harwin and Lucieer (2012) state an optimal GCP distance between $\frac{1}{5}$ and $\frac{1}{10}$ of object distance
31 for UAV applications. Furthermore, the GCPs should be distributed [widely across the target](#)
32 [area \(Smith et al., 2015\) and](#) at the edge or outside the study ~~areareach~~ [reach](#) (James and Robson,
33 2012) to enclose the area of interest, because if the study ~~reacharea~~ [reach](#) is extended outside the

1 GCP area, a significant increase of error is observable in that region (Smith et al., ~~2014,~~
2 ~~Javernick et al., 2014, Rippin et al., 2015~~ 2014, Javernick et al., 2014, Rippin et al., 2015). If
3 data acquisition is performed with parallel-axis UAV images and GCPs are implemented for
4 model refinement, rules for GCP setup according to classical photogrammetry apply, i.e.
5 dense GCP installation around the area of interest and height control points in specific
6 distances as function of image number (more detail in e.g. Kraus, 2007).

7 The measurement of GCPs can be performed either within the point cloud or the images,
8 preferring the latter because identification of distinct points in 3D point clouds of varying
9 density can be less reliable (James and Robson, 2012, Harwin and Lucieer, 2012) compared to
10 sub-pixel measurement in 2D images, where accuracy of GCP identification basically
11 depends on image quality. Fig. 5 a illustrates that only few studies measured GCPs in point
12 clouds producing higher errors compared to other applications at the same distance.

13 **5.32 Errors due to accuracy/precision assessment technique**

14 *Reference of superior accuracy*

15 It is difficult to find a suitable reference for error assessment of SfM photogrammetry in geo-
16 scientific or geomorphologic applications due to the usually complex and rough nature of the
17 studied surfaces. So far, either point based or area based measurements are carried out. On the
18 one hand, point based methods (e.g. RTK GPS or total station) ensure superior accuracy but
19 lack sufficient area coverage for precision statements of local deviations; on the other hand,
20 area based (e.g. TLS) estimations are used, which provide enough data density but can lack of
21 sufficient accuracy (Eltner and Schneider, 2015). Roughness is the least constrained error
22 within point clouds (Lague et al., 2013) independent from the observation method. Thus, it is
23 difficult to distinguish between method noises and actual signal of method differences,
24 especially at scales where the reference method reaches its performance limit. For instance
25 Tonkin et al. (2014) indicate that the quality of total station points is not necessarily superior
26 on steep terrain.

27 Generally, 75 % of the investigations reveal a measured error that is ~~lower than~~ 20 times
28 higher than the ~~reference-error- of the reference~~. But the median shows that ~~superior~~the
29 superiority of the reference ~~accuracy-assessment~~ is actually significantly poorer; the measured
30 error (~~measured error divided by reference accuracy~~) is merely twice the reference error
31 (Fig. 4 c). The reviewed studies further indicate that the superior accuracy of the reference
32 seems ~~scale-dependent~~ to depend on the camera-to-object distance (Fig. 95 b). In shorter
33 distances (below 50 m) most references reveal accuracies that are lower than one magnitude

1 superiority to the measured error. However, alternative reference methods are yet absent.
2 Solely, for applications in further distances the references are sufficient. These findings are
3 relevant for the interpretation of the [relative error-ratio](#) because low ratios at small scale
4 reaches might be due to the low performance of the reference rather than the actual 3D
5 reconstruction quality but due to the reference noise lower errors are not detectable. Low ~~error~~
6 [ratios/relative errors](#) are measured where the superior accuracy is also low (distance 5-50 m)
7 and large ratios are given at distance where superior accuracy increases as well.

8 *Type of deviation measurement*

9 The reviewed studies use different approaches to measure the distance between the reference
10 and the 3D reconstructed [DEM/surface](#). Comparison are either performed in 2.5D (raster) or
11 real 3D (point cloud). Lague et al. (2013) highlight that the application of raster inherits the
12 disadvantage of data interpolation, especially relevant for rough surfaces or complex areas
13 (e.g. undercuts as demonstrated for gullies by Frankl et al., 2015). In this context it is
14 important to note that lower errors are measured for point-to-point distances rather than raster
15 differencing (Smith and Vericat, 2015, Gómez-Guérrez et al., 2014b).

16 Furthermore, within 3D evaluation different methods for deviation measurement exist. The
17 point-to-point comparison is solely suitable for a preliminary error assessment because this
18 method is prone to outliers and differing point densities. By point cloud interpolation alone
19 (point-to-mesh), this issue is not solvable because there are still problems at very rough
20 surfaces (Lague et al., 2013). Different solutions have been proposed: On the one hand,
21 Abellan et al. (2009) proposed averaging the point cloud difference along the spatial
22 dimension, which can also be extended to 4D (x, y, z, time; Kromer et al., 2015). On the other
23 hand, Lague et al. (2013) proposed the M3C2 algorithm for point cloud comparison that
24 considers the local roughness and further computes the statistical significance of detected
25 changes. Stumpf et al. (2014) and Gómez-Gutiérrez et al. (2015) illustrated lower error
26 measurements with M3C2 compared to point-to-point or point-to-mesh. Furthermore, Kromer
27 et al. (2015) showed how the 4D filtering, when its implementation is feasible, allows to
28 considerably increase the level of detection compared to ~~M3C2~~ [other well-established](#)
29 [techniques of comparison](#).

30 **5.43 Standardised error assessment**

31 To compare the achieved accuracies and precisions of different studies a standardised error
32 assessment is necessary. ~~In this review, besides actual measured error comparison, theoretical~~
33 ~~errors for the convergent image configuration are calculated (Eq. 1, Fig. 10) to compare if~~

applications in the field achieved photogrammetric accuracy (Luhman et al., 2014), e.g. considering the theoretical error ratio. The calculation of the theoretical error for the convergent image acquisition schemes is possible, making some basic assumptions about the network geometry, i.e. the strength of image configuration equals 1 (as in James & Robson, 2012), the number of images equals 3 (as in James & Robson, 2012) and an image measurement error of 0.29 due to quantisation noise (as a result of continuous signal conversion to discrete pixel value). However, it is not possible to evaluate the theoretical error for parallel-axes case studies because information about the distance between subsequent images (base) is mostly missing. However, but essential to solve the equation and should not be assumed. Eltner and Schneider (2015) and Eltner et al. (2015) compare their results to parallel-axes theoretical error and could demonstrate that for soil surface measurement from low flying heights at least photogrammetric accuracy is possible. (e.g. sub-cm error for altitudes around 10 m).

(1)

Being:

$$\begin{aligned}
 & \sigma_c \dots \text{coordinate error,} \\
 & q \dots \text{strength of image configuration (set to 1, according to James and Robson, 2012),} \\
 & k \dots \text{number of images (set to 3, according to James and Robson, 2012),} \\
 & ;
 \end{aligned}$$

The results from James and Robson (2012), which show a less reliable performance of SfM than expected from photogrammetric estimation, can be confirmed by the reviewed studies. Image-based 3D reconstruction, considering SfM workflows, perform performs poorer than the theoretical error (Fig. 95c). The measured error is always higher and on average 90 times worse than the theoretical error. Even for the smallest theoretical error ratio the actual error is 6 times higher. Furthermore, it seems that with increasing distance theoretical and measured errors converge slightly.

As demonstrated, diverse factors influence SfM photogrammetry performance and subsequent DEM error with different sensitivity. Generally, accurate and extensive data acquisition is necessary to minimise error significantly (Javernick et al., 2014). Independent reference sources, such as TLS, are not replaceable (James and Robson, 2012) due to their differing error properties (i.e. error reliability) compared to image-matching (Grün, 2012). Synergetic effects of SfM and classical photogrammetry should be used, i.e. benefiting from the high automation of SfM to retrieve initial estimates without any prior knowledge about the image

1 scene and acquisition configuration and adjacent reducing error by approved photogrammetric
2 approaches, which are optimised for high accuracies.

3 The reviewed studies indicate the necessity of a standardised protocol for error assessment
4 because the variety of studies inherit a variety of scales worked at, software used, GCP types
5 measured, deviation measures applied, image network configurations implemented, cameras
6 and platforms operated and reference utilised, making it very difficult to compare results with
7 consistency. Relevant parameters for a standard protocol are suggested in Table 45.

8

9 **56 Perspectives and limitations**

10 SfM photogrammetry has allowed capturing massive three-dimensional datasets by non-
11 specialists during the last five years, and it is highly expected that this technique will evolve
12 during the forthcoming yearsdecade. Current studies are focusing intoon capturing the
13 terrain's geometry with high precision, but several opportunities~~for using point clouds~~ to
14 improve our understanding, modelling and prediction of different earth surface processes still
15 remain unexplored. ~~In return~~For instance, the use of super-macro imagery in conventional
16 SfM workflows is expected to be explored soon for investigating natural phenomena in a
17 much higher level of detail. Nevertheless, some ~~technical and operational aspects are still~~
18 ~~limiting our ability to acquire datasets over naturally complex outcrops. Some~~technological
19 issues that need to be addressed include the progressive degradation of the data quality at
20 ~~longer~~very short distances, due to the effect of a limited depth of field~~on the~~; Up to our
21 knowledge, the use of focus stacking for extending shallow depth of field of single images has
22 not been explored yet. Some other technical and operational aspects are still limiting our
23 ability to derive 3D point cloud-quality, clouds from digital imagery over naturally complex
24 outcrops. Examples include the occurrence of biases and occlusions that can strongly
25 influence the quality of the acquired datasets, and the ~~use~~progressive reduction of ~~super-~~
26 ~~macro and super-zoom lenses for investigating unexplored natural phenomena, between~~
27 ~~others~~the ground resolution (meter/pixel) at longer distances, which can be addressed using
28 mobile platforms such as UAV systems. Eventually, SfM photogrammetry technique may
29 become a mainstream procedure in geomorphological studies during the next decade,
30 perspectives include efforts in cross-disciplinarity, process automatisation, data and code
31 sharing, real time data acquisition and processing, unlocking the archives, etc., as follows:

32 **6.1 Cross-disciplinarity**

1 A great potential relies on adapting three dimensional methods originally developed for the
2 treatment of 3D LiDAR data to investigate natural phenomena through SfM photogrammetry
3 techniques. Applications, [on 3D point cloud treatment](#) dating back from the last decade, ~~must~~
4 [will soon](#) be integrated into SfM photogrammetry post-processing; Examples include:
5 geomorphological investigations in high mountain areas (Milan et al., 2007), geological
6 mapping (Buckley et al., 2008; Franceschi et al. 2009), soil erosion studies (Eltner and
7 Baumgart, 2015), investigation of fluvial systems (Heritage and Hetherington, 2007, Cavalli
8 et al., 2008; Brasington et al., 2012), and mass wasting phenomena (Lim et al., 2005,
9 Oppikofer et al. 2009, Abellan et al., 2010).

10 ~~More specifically, several~~ [Some other](#) data treatment techniques [that](#) have been developed
11 during the last decade ~~for different situations, which~~ [and that](#) will ~~need to be known,~~ adapted
12 and enriched by the growing SfM photogrammetry community; ~~Examples~~ include: automatic
13 lithological segmentation according to the intensity signature (Humair et al., 2015),
14 integration of ground based LiDAR with thermal/hyperspectral imaging for lithological
15 discrimination (Kääb, 2008, Hartzell et al., 2014), extraction of the structural settings on a
16 given outcrop (Jaboyedoff et al., 2007, Sturzenegger and Stead, 2009, Gigli and Casagli,
17 2011, Riquelme et al., 2014), ~~;) and the~~ automatic extraction of [geological patterns such as](#)
18 surface roughness (Poropat, 2009) ~~of the~~, discontinuity spacing/persistence/waviness (Fekete
19 et al. 2010, Khoshelham et al., 2011, Pollyea and Fairley, 2011), ~~;) .~~ [Concerning 4D data](#)
20 [treatment for investigating changes on natural slope, some lessons learned may be adapted](#)
21 [from the](#) bi- and three-dimensional tracking of mass movements (Teza et al., 2007, Monserrat
22 and Crosetto 2008), investigation of progressive failures (Royan et al., 2015, Kromer et al.,
23 2015), and [from the](#) usage of mobile systems (Lato et al., 2009, Michoud et al., 2015).

24 **6.2 Process-automatisation**

25 Handling huge databases is an important issue and although fully automatic techniques may
26 not be necessary [in some applications](#), a series of tedious and manual processes are still
27 required for data treatment.

28 **[6.3 Data and code sharing](#)**

29 [Open data in geomorphometric studies using point clouds is also needed.](#) The development of
30 open-source software for handling huge 3D datasets such as CloudCompare (Girardeau-
31 Montaut, 2015) has considerably boosted ~~geomorphological~~ [geomorphometric](#) studies using
32 3D point clouds. Nevertheless, [apart from the above mentioned case](#), sharing the source code

1 [or the RAW data](#) of specific applications for investigating earth surface processes is still
2 [scarce](#).

3 **6.3 ~~Data and code sharing~~**

4 ~~Open data~~not well established in ~~geomorphological studies using point clouds is also needed~~.
5 ~~Again, our discipline~~. A series of [freely available](#) databases exist for LiDAR datasets
6 (openTopography.org, rockbench.com, 3D-landslide.com). But up to the knowledge of these
7 authors, there is no specific Git-Hub cluster or website dedicated to the maintaining and
8 development of open-access software in geosciences

9 **6.4 Unlocking the archive**

10 The appraisal of digital photography and the exponential increase of data storage capabilities
11 have enabled the massive archive of optical images around the world. Accessing ~~to~~ such
12 quantity of information could provide unexpected opportunities for the four dimensional
13 research of geomorphological processes using SfM photogrammetry workflows. Except for
14 some open repositories (e.g. Flickr, Google street view) the possibility to access the massive
15 optical data is still scarce. In addition, accessing to such databases may become a challenging
16 task due to data interchangeability issues. A considerable effort may be necessary for creating
17 such database with homogeneous data formats and descriptors (type of phenomenon, temporal
18 resolution, pixel size, accuracy, distance to object, existence of GCPs, etc.) during the
19 forthcoming years.

20 A first valuable approach to use data from online imagery was presented by Martin-Brualla et
21 al. (2015), who pave the way for further research in a new field of 3D surface analysis (i.e.
22 time-lapse). Other possible applications might unlock the archive of [ancient](#) airborne,
23 helicopter-based or terrestrial imagery, ranging from the estimation of coastal retreat rates,
24 the observation of the evolution of natural hazards to the monitoring of glacier fronts, and
25 further.

26 **6.5 Real time data acquisition**

27 Rapid developments in automatisisation (soft- and hardware wise) allow for in situ data
28 acquisition and its immediate transfer to processing and analysing institutions. Thus, extreme
29 events are recognisable during their occurrence and authorities or rescue teams can be
30 informed in real-time. In this context SfM photogrammetry could help to detect and quantify
31 rapid volume changes of e.g. glacier fronts, pro-glacial lakes, rock failures and ephemeral
32 rivers.

1 Furthermore, real-time crowd sourcing offers an entirely new dimension of data acquisition.
2 Due to the high connectivity of the public through smartphones, various possibilities arise to
3 share data (Johnson-Roberson et al., 2015). An already implemented example is real-time
4 traffic information. Jackson and Magro (2015) name further options. Crowd sourced imagery
5 can largely expand possibilities to 3D information.

6 **6.6 Time-lapse photography**

7 A limited frequency of data acquisition increases the likelihood of superimposition and
8 coalescence of geomorphological processes (Abellan et al., 2014). Since time-lapse SfM
9 photogrammetry data acquisition has remained so far unexplored, a great prospect is expected
10 on this topic during the coming years. [To date solely James and Robson \(2014b\) demonstrated](#)
11 [its potential by monitoring a lava flow at minute intervals for 37 minutes.](#) One reason why
12 time-lapse SfM photogrammetry remains rather untouched in geosciences lies in the complex
13 nature of producing continuous data sets.

14 Besides the need for an adequate research site (frequent morphodynamic activity), other
15 aspects have to be taken into account: an automatic camera setup is required with self-
16 contained energy supply (either via insolation or wind), adequate storage and appropriate
17 choice of viewing angles onto the area of interest. Furthermore, cameras need to comprise
18 sufficient image overlap and have to be synchronised. Ground control is required and an
19 automatic pipeline for large data treatment should be developed.

20 New algorithms are necessary to deal with massive point cloud databases. Thus, innovative
21 four dimensional approaches have to be developed to take advantage of the information
22 contained in real-time and/or time-lapse monitoring. Combining these datasets with climatic
23 information can improve the modelling of geomorphological processes.

24 **6.7 Automatic UAV surveying ~~(no human controller)~~**

25 Unmanned airborne vehicles already show a large degree of automatisisation as they follow
26 flight paths and acquire data autonomously. Human control is not required except for
27 launching of the multi-copter or fixed wing system. Automatic landing is already provided by
28 several systems. In near future a fully automatic UAV installation could comprise the
29 following: repeated survey of an area of interest, landing and charging at a base station, data
30 link for local storage or satellite based data transfer, and safety mechanism for preventing lift-
31 off during inappropriate weather conditions. However, a large limitation for such realisation
32 lies in legal restrictions because national authorities commonly request for visual contact to

1 the UAV in case of failure. But in remote areas installation of an automatic system could
2 already be allowed by regulation authorities.

3 4 **6—Conclusion**

5 **6.8 Direct geo-referencing**

6 The use of GCPs is very time-consuming in the current SfM workflow. At first, field efforts
7 are high to install and measure the GCPs during data acquisition. Afterwards, again much
8 time and labour is required during post-processing in order to identify the GCPs in the
9 images, although some progress is made regarding to automatic GCP identification, e.g. by
10 the exploitation of templates (Chen et al., 2000). The efficiency of geo-referencing can be
11 increased significantly applying direct geo-referencing. Thus, the location and position of the
12 camera is measured in real time and synchronised to the image capture by an on-board GPS
13 receiver and IMU (inertial measurement unit) recording camera tilts. This applies to UAV
14 systems as well as terrestrial data acquisition, e.g. by smartphones (Masiero et al., 2014).
15 Exploiting direct geo-referencing can reduce usage of GCPs to a minimum or even replace it,
16 which is already demonstrated by Nolan et al. (2015), who generated DEMs with spatial
17 extents of up to 40 km² and a geo-location accuracy of ± 30 cm.

18 The technique can be very advantageous when it comes to monitoring areas with great spatial
19 extents or inaccessible research sites. However, further development is necessary, thereby
20 focusing on light-weighted but precise GPS receivers and IMU systems; on UAVs due to their
21 limited payload and for hand-held devices due to their feasibility (e.g. Eling et al., 2015).

22 23 24 **7 Conclusions**

25 This review has shown the versatility and flexibility of the evolvingrecently established
26 method SfM photogrammetry, which is recapitulated in Fig. 11. Due to its beneficial qualities,
27 a wide community of geoscientists starts to implement 3D reconstruction based on images
28 within a variety of studies. Summing up the publications, there are no considerable
29 disadvantages mentioned (e.g. accuracy wise) compared to other methods that cannot be
30 counteracted by placement of GCPs, camera calibration or a high image number. Frontiers in
31 geomorphometry have been expanded once more, as limits of other surveying techniques such

1 as restricted mobility, isolated area of application and high costs are overcome by the SfM
2 photogrammetry. Its major advantages lie in easy-to-handle and cost-efficient digital cameras
3 as well as non-commercial software solutions.

4 ~~Performance analysis revealed the suitability of SfM photogrammetry at a large range of~~
5 ~~scales in regard to case study specific accuracy necessities. SfM photogrammetry is already~~
6 ~~becoming an essential tool for digital surface mapping. It is employable in a fully automatic~~
7 ~~manner but individual adjustments can be conducted to account for each specific case study~~
8 ~~constraint and accuracy requirement in regard to the intended application. Due to the~~
9 ~~possibility of different degrees of process interaction, non-experts can utilise the method~~
10 ~~depending on their discretion.~~

11 While research of the last years mainly focussed on testing the applicability of SfM
12 photogrammetry in various geo-scientific applications, recent studies try to pave the way for
13 future usages and develop new tools, setups or algorithms. ~~Performance analysis revealed the~~
14 ~~suitability of SfM photogrammetry at a large range of scales in regard to case study specific~~
15 ~~accuracy necessities.~~ However, different factors influencing final DEM quality still need to be
16 addressed. This should be performed under strict experimental (laboratory) designs because
17 complex morphologies, typical in earth surface observations, impede accuracy assessment due
18 to missing superior reference. Thus, independent references and GCPs are still needed in SfM
19 photogrammetry for reliable estimation of the quality of each 3D reconstructed surface.

20
21 Fast and ~~faile~~straightforward generation of ~~DEM~~DEMs using freely available tools produces
22 new challenges. The exploitation of the entire information of the SfM photogrammetry output
23 (3D point cloud or mesh instead of 2.5D raster) will become a significant ~~issue~~challenge in
24 future studies of high resolution topography (Passalacqua et al., 2015), which has to be even
25 extended to 4D when ~~additionally considering~~investigating the evolution along time. Thus,
26 especially comprehensive end user software needs further progress in these aspects.

27 ~~Nevertheless, SfM photogrammetry is already becoming an essential tool for digital surface~~
28 ~~mapping. It is employable in a fully automatic manner but individual adjustments can be~~
29 ~~conducted to account for each specific case study constraint and accuracy requirement in~~
30 ~~regard to the intended application. Due to the possibility of different degrees of process~~
31 ~~interaction, non-experts can utilise the method depending on their discretion.~~

1 **Appendix A:**

2 [Table summarises Summary of](#) information about reviewed studies used for application evaluation and performance assessment of SfM
 3 photogrammetry. [Variables are explained in chapter 5.](#)

ID	Author	Year	Application	Software	Perspective	Distance [m]	Scale* [m]	Pixel size [μm]	Image number	Complexity of SfM tool	Measurement error [mm]	Relative error	referen superi
1	Castillo et al.	2012	gully erosion	Bundler + PMVS2	terrestrial	7	7	5.2	191	basic	20	350	-
2	Castillo et al.	2014	ephemeral gully erosion	Bundler + PMVS2	terrestrial	6	25	5.2	515	basic	22	273	11
3	Castillo et al.	2015	gully erosion	SF3M	terrestrial	10	350	1.5	3095	basic	69	145	3.45
4	Dietrich	2016	riverscape mapping	PhotoScan	helicopter	200	10000	4.3	1483	complex	730	274	-
5	Eltner et al.	2015	soil erosion	Pix4D	UAV	10	30	2.0, 5.0	100	complex	5, 6	2000, 1667	-
6	Eltner and Schneider	2015	soil roughness	VisualSfM + PMVS2, PhotoScan, Pix4D, APERO + MicMac, Bundler + PMVS2	UAV	12	15	5.0	13	basic, complex	8.1 - 9.8	1224 - 1481	-
7	Favalli et al.	2012	geological outcrops, volcanic bomb,	Bundler + PMVS2	terrestrial	1	0.1 - 0.3	5.2	30 - 67	basic	0.3 - 3.8	367 - 3333	-

8	Fonstad et al.	2013	stalagmite bedrock channel and floodplain	Photosynth (Bundler implementation) PhotoScan	terrestrial	40	200	1.7	304	basic	250	160	2
9	Frankl et al.	2015	gully measurement	PhotoScan	terrestrial	2	10	5.2	180 - 235	complex	17 - 190	11 - 147	0 - 4
10	Genchi et al.	2015	bioerosion pattern	VisualSfM + PMVS2	UAV	20	100	1.5	400	basic	35	571	-
11	Gómez-Gutiérrez et al.	2014	gully headcut	123D catch	terrestrial	9.3 - 10.5	10	4.3	41 - 93	basic	12 - 32	291 - 792	-
12	Gómez-Gutiérrez et al.	2014	rock glacier	123D catch	terrestrial	300	130	8.2	6	basic	430	698	72
13	Gómez-Gutiérrez et al.	2015	rock glacier	123D catch, PhotoScan	terrestrial	300	130	8.2	9	basic, complex	84 - 1029	-	-
14	Immerzeel et al.	2014	dynamic of debris covered glacial tongue	PhotoScan	UAV	300	3500	1.3	284, 307	complex	330	909	-
15	James and Robson	2012	volcanic bomb, summit crater, coastal cliff	Bundler + PMVS2	terrestrial, UAV	0.7 - 1000	0.1 - 1600	5.2, 7.4	133 - 210	basic	1000 - 2333	0 - 62	1 - 12
16	Javernick et al.	2014	braided river	PhotoScan	helicopter	700	1500	-	147	complex	170	4118	3
17	Johnson et al.	2014	alluvial fan, earthquake scarp	PhotoScan	UAV	50, 60	300, 1000	4.8	233. 450	complex	130 - 410	122 - 385	-

18	Kaiser et al.	2014	gully and rill erosion	PhotoScan	terrestrial	5	10	6.4	-	complex	73 - 141	35 - 68	-
19	Leon et al.	2015	coral reef roughness	PhotoScan	terrestrial (marine)	1.5	250	1.5	1370	complex	0.6	2500	-
20	Mancini et al.	2013	fore dune	PhotoScan	UAV	40	200	4.3	550	complex	110 - 190	211 - 364	4
21	Micheletti et al.	2014	river bank, alluvial fan	123D Catch	terrestrial	10, 345	10, 300	4.8, 1.8	13	complex	16.8 - 526.3	327 - 595	-
22	Nadal-Romero et al.	2015	badland erosion	PhotoScan	terrestrial	50, 125	50, 100	5.5	15, 17	complex	14 - 33	2500 - 4032	1 - 2
23	Nouwakpo et al.	2015	microtopography erosion plots	PhotoScan	terrestrial	2	6	6.4	25	complex	5	400	-
24	Ouédraogo et al.	2014	agricultural watershed	Apero + MicMac, PhotoScan	UAV	100	200	2.0	760	complex	90, 139	1111, 719	-
25	Piermattei et al.	2015	debris covered glacier monitoring	PhotoScan	terrestrial	100	350	4.8, 6.3	35, 47	complex	300, 130	333, 769	2, 1
26	Prosdocimi et al.	2015	channel bank erosion	PhotoScan	terrestrial	7	30	1.4 - 6.3	60	complex	57 - 78	90 - 123	1
27	Rippin et al.	2015	supra-glacial hydrology	PhotoScan	UAV	121	2000	2.2	423	complex	400	303	-
28	Ruzic et al.	2014	coastal cliff	Autodesk ReCap	terrestrial	15	50	2.0	250	basic	70	214	1
29	Smith et al.	2014	post-flash flood evaluation	PhotoScan	terrestrial	50	150	1.7	-	complex	135	370	14
30	Smith and	2015	badland changes	PhotoScan	terrestrial,	5 - 250	20 -	1.7,	30 -	complex	12.8 - 445	132 - 974	2 - 89

43	Bretar et al.	2013	erosion/abrasion (volcanic) surface roughness	APERRO + MicMac	terrestrial	1.5	5.9 - 24.6	-	-	-	-	-	-
44	Brothelande et al.	2015	post-caldera resurgence	PhotoScan	aircraft	150	6000	8.2	7000	-	3100	48	62
45	Burns et al.	2015	coral reef	Photoscan	terrestrial (marine)	2	28	-	-	-	-	-	-
46	Clapuyt et al.	2015	slope morphology	VisualSFM	UAV	50	100	-	-	-	-	-	-
47	Dall'Asta et al.	2015	rock glacier monitoring	APERRO + MicMac, Photoscan	UAV	150		-	-	-	-	-	-
48	Dandois and Ellis	2013	vegetation mapping	Photoscan	UAV	130	250	-	-	-	-	-	-
49	Fernández et al.	2015	landslide	Photoscan	UAV	90	250	-	-	-	-	-	-
50	Gienko and Terry	2014	coastal boulders	Photoscan	terrestrial	3	2.5	-	-	-	-	-	-
51	Fugazza et al.	2015	glacier mapping	Menci APS	UAV	250	500	-	-	-	-	-	-
52	Gomez	2014	volcano morphology	Photoscan	aircraft	-	10000	-	-	-	-	-	-
53	Harwin and Lucieer	2012	coastal erosion	Bundler + PMVS2	UAV	120	100	-	1	-	-	-	-
54	James and Varley	2012	volcanic dome control	Bundler Photogrammetry package	aircraft	505 – 2420	250	-	-	-	-	-	-
55	Kaiser et al.	2015	soil hydraulic	PhotoScan	terrestrial	0.5	1	-	-	-	-	-	-

56	Lucieer et al.	2013	roughness landslide	PhotoScan	UAV	40	125	-	-	-	-	-	-
57	Lucieer et al.	2014	antartic moss beds	PhotoScan	UAV	50	64	-	-	-	-	-	-
58	Meesuk et al.	2014	Urban flooding	VisualSfM	terrestrial	-	-	-	-	-	-	-	-
59	Morgenroth and Gomez	2014	tree structure	Photoscan	terrestrial	5	5	-	-	-	-	-	-
60	Nouwakpo et al.	2014	soil microtopography	Photoscan	terrestrial	3.1	10	-	-	-	-	-	-
61	Stöcker et al.	2015	gully erosion	APER0 + MicMac	terrestrial + UAV	2 + 15	35	-	-	-	-	-	-
62	Ryan et al.	2015	glacier drainage observation	Photoscan	UAV	500	5000	-	-	-	-	-	-
63	Torres-Sánchez et al.	2015	tree plantation	Photoscan	UAV	50, 100	-	-	-	-	-	-	-
64	Turner et al.	2015	landslide monitoring	Bundler + PMVS2	UAV	50	-	-	-	-	-	-	-
65	Vasuki et al.	2014	structural geology	Bundler + PMVS2	UAV	30 - 40	100	-	-	-	-	-	-

1

2 **These studies are considered for performance analysis.**

3 *For most authors not all camera parameters are given. Hence, camera parameters are retrieved from dpreview.com (or similar sources).*

4 * If scale or distance is not given, they are estimated from study area display.

1 | **Appendix B:**

2 | ~~Table summarises non-commercial software tools beneficial for SfM photogrammetry processing and post-processing.~~

1 **Acknowledgements**

2 The authors A. Eltner, A. Kaiser and F. Neugirg are funded by the German Research
3 Foundation (DFG) (MA 2504/15-1, HA5740/3-1, SCHM1373/8-1). A. Abellan acknowledges
4 [funding support](#) by [the Risk Analysis group](#) (Univ. Lausanne) and the [UPC](#) (RockRisk
5 research project (BIA2013-42582-P)).

6 [We would like to thank an anonymous referee and Matt Westoby for their remarks, which](#)
7 [significantly improved the manuscript.](#)

9 **References**

10 Abellán, A., Jaboyedoff, M., Oppikofer, T. and Vilaplana, J. M.: Detection of millimetric
11 deformation using a terrestrial laser scanner: experiment and application to a rockfall event,
12 *Nat. Hazard Earth Sys.*, 9, 365–372, 2009.

13 Abellán, A., Calvet, J., Vilaplana, J. M. and Blanchard, J.: Detection and spatial prediction of
14 rockfalls by means of terrestrial laser scanner monitoring, *Geomorphology*, 119, 162–171,
15 doi:10.1016/j.geomorph.2010.03.016, 2010.

16 Abellán, A., Oppikofer, T., Jaboyedoff, M., Rosser, N. J., Lim, M. and Lato, M. J.: Terrestrial
17 laser scanning of rock slope instabilities, *Earth Surf. Proc. Landf.*, 39(1), 80–97.
18 doi:10.1002/esp.3493, 2014.

19 Ai, M., Hu, Q., Li, J., Wang, M., Yuan, H. and Wang, S.: A Robust Photogrammetric
20 Processing Method of Low-Altitude UAV Images, *Remote Sensing*, 7, 2302–2333,
21 doi:10.3390/rs70302302, 2015.

22 Astre, H.: SfMtoolkit. <http://www.visual-experiments.com/demos/sfmtoolkit/>, last access
23 Nov. 2015.

24 ~~[Bay, H., Ess, A., Tuytelaars, T. and Van Gool, L.: Speeded-Up Robust Features \(SURF\),](#)~~
25 ~~[Comput. Vis. Image Und.](#), 110(3), 346–359, doi:10.1016/j.cviu.2007.09.014, 2008.~~

26 Bemis, S. P., Micklethwaite, S., Turner, D., James, M. R., Akciz, S., Thiele, S. T. and
27 Bangash, H. A.: Ground-based and UAV-Based photogrammetry: A multi-scale, high-
28 resolution mapping tool for structural geology and paleoseismology, *J. Struct. Geol.*, 69, 163–
29 178, doi:10.1016/j.jsg.2014.10.007, 2014.

- 1 Bendig, J., Bolten, A. and Bareth, G.: UAV-based Imaging for Multi-Temporal, very high
2 Resolution Crop Surface Models to monitor Crop Growth Variability, *Photogramm.*
3 *Fernerkun.*, 6, 551–562, doi:10.1127/1432-8364/2013/02001, 2013.
- 4 Bini, M., Isola, I., Pappalardo, M., Ribolini, A., Favalli, M., Ragaini, L. and Zanchetta, G.:
5 Abrasive notches along the Atlantic Patagonian coast and their potential use as sea level
6 markers: the case of Puerto Deseado (Santa Cruz, Argentina), *Earth Surf. Proc. Landf.*, 39,
7 1550–1558, doi:10.1002/esp.3612, 2014.
- 8 Bracken, L. J., Turnbull, L., Wainwright, J. and Bogaart, P.: State of Science Sediment
9 connectivity: a framework for understanding sediment transfer at multiple scales, *Earth Surf.*
10 *Proc. Landf.*, 40, 177–188, doi:10.1002/esp.3635, 2015.
- 11 Brasington, J., Vericat, D. and Rychkov, I.: Modeling river bed morphology, roughness, and
12 surface sedimentology using high resolution terrestrial laser scanning, *Water Resources*
13 *Research*, 48, W11519, doi:10.1029/2012WR012223, 2012.
- 14 Bretar, F., Arab-Sedze, M., Champion, J., Pierrot-Deseilligny, M., Heggy, E. and
15 Jacquemoud, S.: An advanced photogrammetric method to measure surface roughness:
16 Application to volcanic terrains in the Piton de la Fournaise, Reunion Island, *Remote Sens.*
17 *Environ.*, 135, 1–11, doi:10.1016/j.rse.2013.03.026, 2013.
- 18 Brothelande, E., Lénat, J.-F., Normier, A., Bacri, C., Peltier, A., Paris, R., Kelfoun, K., Merle,
19 O., Finizola, A. And Garaebiti, E.: Insights into the evolution of the Yenkahe resurgent dome
20 (Siwi caldera, Tanna Island, Vanuatu) inferred from aerial high-resolution photogrammetry, *J.*
21 *Volcanol. Geoth. Res.*, doi:10.1016/j.jvolgeores.2015.04.006, 2015.
- 22 Brown, M. Z., Burschka, D. and Hager, G. D.: Advances in Computational Stereo, in: *IEEE*
23 *Transactions on pattern analysis and machine intelligence*, 25, 993–1008, 2003.
- 24 Buckley, S., Howell, J., Enge, H. and Kurz, T.: Terrestrial laser scanning in geology: data
25 acquisition, processing and accuracy considerations, *J. Geol. Soc. London*, 165, 625–638,
26 2008.
- 27 Burns, J. H. R., Delparte, D., Gates, R. D. and Takabayashi, M.: Integrating structure-from-
28 motion photogrammetry with geospatial software as a novel technique for quantifying 3D
29 ecological characteristics of coral reefs, *PeerJ*, 3, doi:10.7717/peerj.1077, 2015.
- 30 Castillo, C., Pérez, R., James, M. R., Quinton, J. N., Taguas, E. V. and Gómez, J. A.:
31 Comparing the Accuracy of Several Field Methods for Measuring Gully Erosion, *Soil Sci.*
32 *Soc. Am. J.*, 76, doi:10.2136/sssaj2011.0390, 2012.

- 1 Castillo, C., Taguas, E. V, Zarco-Tejada, P., James, M. R. and Gómez, J. A.: The normalized
2 topographic method: an automated procedure for gully mapping using GIS, *Earth Surf. Proc.*
3 *Landf.*, 39, 2002–2015, doi:10.1002/esp.3595, 2014.
- 4 Castillo, C., James, M. R., Redel-Macías, M. D., Pérez, R. and Gómez, J. A.: SF3M software:
5 3-D photo-reconstruction for non-expert users and its application to a gully network, *SOIL*, 1,
6 583–594, doi:10.5194/soil-1-583-2015, 2015.
- 7 Cavalli, M., Tarolli, P., Marchi, L. and Fontana, G. D.: The effectiveness of airborne LiDAR
8 data in the recognition of channel-bed morphology, *Catena*, 73(3), 249–260,
9 doi:10.1016/j.catena.2007.11.001, 2008.
- 10 Chandler, J.: Effective application of automated digital photogrammetry for
11 geomorphological research, *Earth Surf. Proc. Landf.*, 24, 51–63, 1999.
- 12 [Chen, L. C., Lo, C. Y., Liu, C. L. And Chen, A. J.: Orientation modelling by matching image](#)
13 [templates of a GCP database, *Proc. 21st ACRS*, 21\(2\), 2000.](#)
- 14 Cignoni, P., Callieri, M., Corsini, M., Dellepiane, M., Ganovelli, F. And Ranzuglia, G.:
15 MeshLab: an Open-Source Mesh Processing Tool, in: Eurographics Italian Chapter
16 Conference, Salerno, Italy, 129–136, 2008.
- 17 Clapuyt, F., Vanacker, V. and Van Oost, K.: Reproducibility of UAV-based earth topography
18 reconstructions based on Structure-from-Motion algorithms, *Geomorphology*,
19 doi:10.1016/j.geomorph.2015.05.011, 2015.
- 20 Collier, P.: The impact on topographic mapping of developments in land and air survey:
21 1900-1939, *Cartogr. Geogr. Inform.*, 29(3), 155-174, 2002.
- 22 [Dall’Asta, E., Delaloye, R., Diotri, F., Forlani, G., Fornari, Morro di Cella, U. M.,](#)
23 [Pogliotti, P., Roncella, R. and Santise, M.: Use of UAS in a High Mountain Landscape: the](#)
24 [Case of Gran Sommetta Rock Glacier \(AO\). *ISPRS – Int. Arch. Photogramm. Rem. Sens.*,](#)
25 [XL-3/W3, 391-397, 2015.](#)
- 26 Dandois, J. P. and Ellis, E. C.: High spatial resolution three-dimensional mapping of
27 vegetation spectral dynamics using computer vision, *Remote Sens. Environ.*, 136, 259–276,
28 doi:10.1016/j.rse.2013.04.005, 2013.
- 29 Díaz-Varela, R., de la Rosa, R., León, L. and Zarco-Tejada, P.: High-Resolution Airborne
30 UAV Imagery to Assess Olive Tree Crown Parameters Using 3D Photo Reconstruction:

1 Application in Breeding Trials, *Remote Sensing*, 7, 4213–4232. doi:10.3390/rs70404213,
2 2015.

3 Dietrich, J. T.: Riverscape Mapping with Helicopter-Based Structure-From-Motion
4 Photogrammetry, *Geomorphology*, 252, 144–157, doi:10.1016/j.geomorph.2015.05.008,
5 2016.

6 Ducher, G.: Photogrammetry - The largest operational application of remote sensing,
7 *Photogrammetria*, 41(2), 72-82., 1987.

8 East, A. E., Pess, G. R., Bountry, J. A., Magirl, C. S., Ritchie, A. C., Logan, J. B., Randle, T.
9 J., Mastin, M. C., Minear, J. T., Duda, J. J., Liermann, M. C., McHenry, M. L., Beechie, T. J.
10 and Shafroth, P. B.: Reprint of: Large-scale dam removal on the Elwha River, Washington,
11 USA: River channel and floodplain geomorphic change, *Geomorphology*, 246, 687–708,
12 doi:10.1016/j.geomorph.2015.04.027, 2015.

13 [Eling, C., Wieland, M., Hess, C., Klingbeil, L. and Kuhlmann, H.: Development and](#)
14 [evaluation of a UAV based mapping system for remote sensing and surveying applications,](#)
15 [ISPRS – Int. Arch. Photogramm. Rem. Sens., XL-1/W4, 233-239, 2015.](#)

16 Eltner, A., Mulsow, C. and Maas, H.: Quantitative Measurement of Soil Erosion from Tls and
17 Uav Data, [ISPRS - Int. Arch. Photogramm. Rem. Sens., XL-1/W2](#), 119–124, 2013.

18 Eltner, A. and Baumgart, P.: Accuracy constraints of terrestrial Lidar data for soil erosion
19 measurement: Application to a Mediterranean field plot, *Geomorphology*, 245, 243–254,
20 doi:10.1016/j.geomorph.2015.06.008, 2015.

21 Eltner, A., Baumgart, P., Maas, H.-G. and Faust, D.: Multi-temporal UAV data for automatic
22 measurement of rill and interrill erosion on loess soil. *Earth Surf. Proc. Landf.*, 40(6), 741–
23 755, doi:10.1002/esp.3673, 2015.

24 Eltner, A. and Schneider, D.: Analysis of Different Methods for 3D Reconstruction of Natural
25 Surfaces from Parallel-Axes UAV Images, *Photogramm. Rec.*, 30(151), 279–299,
26 doi:10.1111/phor.12115, 2015.

27 Favalli, M., Fornaciai, A., Isola, I., Tarquini, S. and Nannipieri, L.: Multiview 3D
28 reconstruction in geosciences, *Comput. Geosc.*, 44, 168–176,
29 doi:10.1016/j.cageo.2011.09.012, 2012.

- 1 Fekete, S., Diederichs, M. and Lato, M.: Geotechnical and operational applications for 3-
2 dimensional laser scanning in drill and blast tunnels, *Tunnelling and Underground Space*
3 *Technology*, 25(5), 614–628, doi:10.1016/j.tust.2010.04.008, 2010.
- 4 Fernández, T., Pérez, J. L., Cardenal, F. J., López, A., Gómez, J. M., Colomo, C., Delgado, J.
5 and Sánchez, M.: Use of a Light UAV and Photogrammetric Techniques To Study the
6 Evolution of a Landslide in Jaén (Southern Spain), *ISPRS – Int. Arch. Photogramm. Rem.*
7 *Sens.*, XL-3/W3, 241–248, doi:10.5194/isprsarchives-XL-3-W3-241-2015, 2015.
- 8 ~~Fischler, M. A. and Bolles, R. C.: Random sample consensus: a paradigm for model fitting~~
9 ~~with applications to image analysis and automated cartography, *Commun. ACM*, 24(6), 381–~~
10 ~~395, doi:10.1145/358669.358692, 1981.~~
- 11 Fonstad, M. A., Dietrich, J. T., Courville, B. C., Jensen, J. L. and Carbonneau, P. E.:
12 Topographic structure from motion: a new development in photogrammetric measurement,
13 *Earth Surf. Proc. Landf.*, 38, 421–430, doi:10.1002/esp.3366, 2013.
- 14 Frahm, J.-M., Pollefeys, M., Lazebnik, S., Gallup, D., Clipp, B., Raguram, R., Wu, C., Zach,
15 C. and Johnson, T.: Fast robust large-scale mapping from video and internet photo
16 collections., *ISPRS J. Photogramm.*, 65(6), 538–549, doi:10.1016/j.isprsjprs.2010.08.009,
17 2010.
- 18 Franceschi, M., Teza, G., Preto, N., Pesci, A., Galgaro, A. and Girardi, S.: Discrimination
19 between marls and limestones using intensity data from terrestrial laser scanner, *ISPRS J.*
20 *Photogramm.*, 64(6), 522–528, doi:10.1016/j.isprsjprs.2009.03.003, 2009.
- 21 Francioni, M., Salvini, R., Stead, D., Giovannini, R., Riccucci, S., Vanneschi, C. and Gulli,
22 D.: An integrated remote sensing-GIS approach for the analysis of an open pit in the Carrara
23 marble district, Italy: Slope stability assessment through kinematic and numerical methods,
24 *Comp. Geot.*, 67, 46–63, doi:10.1016/j.compgeo.2015.02.009, 2015.
- 25 Frankl, A., Stal, C., Abraha, A., Nyssen, J., Rieke-Zapp, D., De Wulf, A. and Poesen, J.:
26 Detailed recording of gully morphology in 3D through image-based modelling PhotoScan
27 Digital Elevation Model (DEM) Soil pipes Structure from ~~MotionM~~ otion–Multi View
28 Stereo (SfM–MVS) Volume calculation, *Catena*, 127, 92–101,
29 doi:10.1016/j.catena.2014.12.016, 2014.
- 30 Fugazza, D., Senese, A., Azzoni, R. S., Smiraglia, C. Cernuschi, M. Severi, D. D. and
31 Guglielmina, A.: High-resolution mapping of glacier surface features. The UAV survey of the

1 [Forni glacier \(Stelvio National Park, Italy\), *Geogr. Fis. Dinam. Quat.*, 38, 25-33,](#)
2 [doi:10.4461/GFDQ.2015.38.03, 2015.](#)

3 Furukawa, Y., Curless, B., Seitz, S. M. and Szeliski, R.: Towards Internet-scale multi-view
4 stereo, in: IEEE Conference on Computer Vision and Pattern Recognition, San Francisco,
5 CA, USA, 1434–1441, doi:10.1109/CVPR.2010.5539802, 2010.

6 Furukawa, Y. and Ponce, J.: Accurate, dense, and robust multiview stereopsis, in: IEEE
7 Transactions on Pattern Analysis and Machine Intelligence, 83, 1362–1376,
8 doi:10.1109/TPAMI.2009.161, 2010.

9 Genchi, S. A., Vitale, A. J., Perillo, G. M. E. and Delrieux, C. A.: Structure-from-Motion
10 Approach for Characterization of Bioerosion Patterns Using UAV Imagery, *Sensors*, 15,
11 3593–3609, doi:10.3390/s150203593, 2015.

12 Gienko, G. A. and Terry, J. P.: Three-dimensional modeling of coastal boulders using multi-
13 view image measurements, *Earth Surf. Proc. Landf.*, 39, 853–864, doi:10.1002/esp.3485,
14 2014.

15 Gigli, G. and Casagli, N.: Semi-automatic extraction of rock mass structural data from high
16 resolution LIDAR point clouds., *Int. J. Rock Mech. Min.*, 48, 187–198,
17 doi:10.1016/j.ijrmms.2010.11.009, 2011.

18 Girardeau-Montaut, D.: CloudCompare (version 2.x; GPL software), EDF RandD, Telecom
19 ParisTech, <http://www.cloudcompare.org/>, last access: Mar. 2015.

20 Gomez, C.: Digital photogrammetry and GIS-based analysis of the bio-geomorphological
21 evolution of Sakurajima Volcano, diachronic analysis from 1947 to 2006. *J. Volcanol. Geoth.*,
22 280, 1–13, 2014.

23 Gomez, C., Hayakawa, Y. and Obanawa, H.: A study of Japanese landscapes using structure
24 from motion derived DSMs and DEMs based on historical aerial photographs: New opportu-
25 nities for vegetation monitoring and diachronic geomorphology, *Geomorphology*, 242, 11–20,
26 doi:10.1016/j.geomorph.2015.02.021, 2015.

27 Gómez-Gutiérrez, Á., de Sanjosé-Blasco, J. J., de Matías-Bejarano, J. and Berenguer-
28 Sempere, F.: Comparing Two Photo-Reconstruction Methods to Produce High Density Point
29 Clouds and DEMs in the Corral del Veleta Rock Glacier (Sierra Nevada, Spain), *Remote*
30 *Sensing*, 6, 5407–5427, doi:10.3390/rs6065407, 2014.

1 Gómez-Gutiérrez, Á., Schnabel, S., Berenguer-Sempere, F., Lavado-Contador, F. and Rubio-
2 Delgado, J.: Using 3D photo-reconstruction methods to estimate gully headcut erosion,
3 *Catena*, 120, 91–101, doi:10.1016/j.catena.2014.04.004, 2014.

4 Gómez-Gutiérrez, Á., de Sanjosé-Blasco, J., Lozano-Parra, J., Berenguer-Sempere, F. and de
5 Matías-Bejarano, J.: Does HDR Pre-Processing Improve the Accuracy of 3D Models
6 Obtained by Means of two Conventional SfM-MVS Software Packages? The Case of the
7 Corral del Veleta Rock Glacier, *Remote Sensing*, 7, 10269–10294, doi:10.3390/rs70810269,
8 2015.

9 Gruen, A.: Development and status of image matching in photogrammetry, *Photogramm.*
10 *Rec.*, 27(137), 36–57, doi:10.1111/j.1477-9730.2011.00671.x, 2012.

11 Hartzell, P., Glennie, C., Biber, K., and Khan, S. (2014). Application of multispectral LiDAR
12 to automated virtual outcrop geology. *ISPRS Journal of Photogrammetry and Remote*
13 *Sensing*, 88, 147–155. doi:10.1016/j.isprsjprs.2013.12.004

14 Harwin, S. and Lucieer, A.: Assessing the Accuracy of Georeferenced Point Clouds Produced
15 via Multi-View Stereopsis from Unmanned Aerial Vehicle (UAV) Imagery, *Remote Sensing*,
16 4, 1573–1599, doi:10.3390/rs4061573, 2012.

17 Heritage, G. and Hetherington, D.: Towards a protocol for laser scanning in fluvial
18 geomorphology, *Earth Surf. Proc. Landf.*, 32(32), 66–74, doi:10.1002/esp.1375, 2007.

19 Hirschmüller, H.: Semi-Global Matching – Motivation, Developments and Applications,
20 *Photogrammetric Week*, 11, 173–184, 2011.

21 Humair, F., Abellan, A., Carrea, D., Matasci, B., Epard, J.-L. and Jaboyedoff, M.: Geological
22 layers detection and characterisation using high resolution 3D point clouds: example of a box-
23 fold in the Swiss Jura Mountains, *Eur. J. Rem. Sens.*, 48, 541–568,
24 doi:10.5721/EuJRS20154831, 2015.

25 Immerzeel, W. W., Kraaijenbrink, A., Shea, J. M., Shrestha, A. B., Pellicciotti, F., Bierkens,
26 M. F. P. and De Jong, S. M.: High-resolution monitoring of Himalayan glacier dynamics
27 using unmanned aerial vehicles, *Rem. Sens. Environ.*, 150, 93–103,
28 doi:10.1016/j.rse.2014.04.025, 2014.

29 Jaboyedoff, M., Metzger, R., Oppikofer, T., Couture, R., Derron, M.-H., Locat, J. and Turmel,
30 D.: New insight techniques to analyze rock-slope relief using DEM and 3D- imaging cloud
31 points: COLTOP-3D software. In: *Rock Mechanics: Meeting Society’s Challenges and*

1 Demands, Eberhardt, E., Stead, D. and Morrison, T. (Eds.), 1st ed., Taylor and Francis,
2 London, 61–68, 2007.

3 [Jaboyedoff, M., Oppikofer, T., Abellán, A., Derron, M.-H., Loye, A., Metzger, R. and](#)
4 [Pedrazzini, A.: Use of LIDAR in landslide investigations: a review, *Nat. Hazards*, 61, 5-28,](#)
5 [doi: 10.1007/s11069-010-9634-2, 2012.](#)

6 Jackson, M. and Magro, G.: Real-time crowd-sourcing, data and modelling. In: IAIA15
7 Conference Proceedings, Florence, 2015.

8 James, M. R. and Robson, S.: Straightforward reconstruction of 3D surfaces and topography
9 with a camera: Accuracy and geoscience application, *J. Geoph. Res.*, 117, F03017,
10 doi:10.1029/2011JF002289, 2012.

11 James, M. R. and Varley, N.: Identification of structural controls in an active lava dome with
12 high resolution DEMs: Volcán de Colima, Mexico, *Geoph. Res. Let.*, 39, L22303,
13 doi:10.1029/2012GL054245, 2012.

14 James, M. R. and Robson, S.: Mitigating systematic error in topographic models derived from
15 UAV and ground-based image networks, *Earth Surf. Proc. Landf.*, 39, 1413–1420,
16 doi:10.1002/esp.3609, 2014.

17 James, M. R. and Robson, S.: Sequential digital elevation models of active lava flows from
18 ground-based stereo time-lapse imagery, *ISPRS J. Photogramm. Rem. Sens.*, 97, 160–170,
19 doi:10.1016/j.isprsjprs.2014.08.011, 2014.

20 Javernick, L., Brasington, J. and Caruso, B.: Modeling the topography of shallow braided
21 rivers using Structure-from-Motion photogrammetry, *Geomorphology*, 213, 166–182,
22 doi:10.1016/j.geomorph.2014.01.006, 2014.

23 Johnson, K., Nissen, E., Saripalli, S., Arrowsmith, J. R., McGarey, P., Scharer, K., Williams,
24 P. and Blisniuk, K.: Rapid mapping of ultrafine fault zone topography with structure from
25 motion, *Geosphere*, 10(5), doi:10.1130/GES01017.1, 2014.

26 Johnson-Roberson, M., Bryson, M., Douillard, B., Pizarro, O. and Williams, S. B.:
27 Discovering salient regions on 3D photo-textured maps: Crowdsourcing interaction data from
28 multitouch smartphones and tablets, *Comput. Vis. Image Und.*, 131, 28–41,
29 doi:10.1016/j.cviu.2014.07.006, 2015.

1 Kääb, A.: Glacier Volume Changes Using ASTER Satellite Stereo and ICESat GLAS Laser
2 Altimetry. A Test Study on Edgeøya, Eastern Svalbard, *IEEE Transactions on Geoscience
3 and Remote Sensing*, 46(10), 2823 – 2830, doi:10.1109/TGRS.2008.2000627, 2008.

4 Kääb, A., Girod, L. and Berthling, I.: Surface kinematics of periglacial sorted circles using
5 structure-from-motion technology, *The Cryosphere*, 8, 1041–1056, doi:10.5194/tc-8-1041-
6 2014, 2014.

7 Kaiser, A., Neugirg, F., Rock, G., Müller, C., Haas, F., Ries, J., and Schmidt, J.: Small-Scale
8 Surface Reconstruction and Volume Calculation of Soil Erosion in Complex Moroccan Gully
9 Morphology Using Structure from Motion, *Remote Sensing*, 6, 7050–7080,
10 doi:10.3390/rs6087050, 2014.

11 Kaiser, A., Neugirg, F., Haas, F., Schmidt, J., Becht, M. and Schindewolf, M.: Determination
12 of hydrological roughness by means of close range remote sensing, *SOIL*, 1, 613–620,
13 doi:10.5194/soil-1-613-2015, 2015.

14 Khoshelham, K., Altundag, D., Ngan-Tillard, D. and Menenti, M.: Influence of range
15 measurement noise on roughness characterization of rock surfaces using terrestrial laser
16 scanning, *Int. J. Rock Mech. Min.*, 48, 1215–1223, doi:10.1016/j.ijrmms.2011.09.007, 2011.

17 Kraus, K.: *Photogrammetry: Geometry from Images and Laser Scans*, 2nd edition, De
18 Gruyter, Berlin, Germany, 459 pages, 2007.

19 Kromer, R., Abellán, A., Hutchinson, D., Lato, M., Edwards, T. and Jaboyedoff, M.: A 4D
20 Filtering and Calibration Technique for Small-Scale Point Cloud Change Detection with a
21 Terrestrial Laser Scanner, *Remote Sensing*, 7(10), 13029–13052, doi:10.3390/rs71013029,
22 2015.

23 Lague, D., Brodu, N., and Leroux, J.: Accurate 3D comparison of complex topography with
24 terrestrial laser scanner: Application to the Rangitikei canyon (N-Z), *ISPRS J. Photogramm.
25 Rem. Sens.*, 82, 10–26, doi:10.1016/j.isprsjprs.2013.04.009, 2013.

26 Laussedat, A.: *La métrophotographie*, Bibliothèque Photographique, Gauthier-Villars, Paris,
27 55 pages, 1899.

28 Lato, M., Hutchinson, J., Diederichs, M., Ball, D. and Harrap, R.: Engineering monitoring of
29 rockfall hazards along transportation corridors: using mobile terrestrial LiDAR, *Nat. Hazard
30 Earth Sys.*, 9, 935–946, 2009.

- 1 Leon, J. X., Roelfsema, C. M., Saunders, M. I. and Phinn, S. R.: Measuring coral reef terrain
2 roughness using “Structure-from-Motion” close-range photogrammetry, *Geomorphology*,
3 242, 21–28, doi:10.1016/j.geomorph.2015.01.030, 2015.
- 4 Lim, M., Petley, D. N., Rosser, N. J., Allison, R. J., Long, A. J. and Pybus, D.: Combined
5 digital photogrammetry and time-of-flight laser scanning for monitoring cliff evolution,
6 *Photogramm. Rec.*, 20(110), 109–129, 2008.
- 7 ~~[Lowe, D. G.: Object recognition from local scale invariant features, The Proceedings of the](#)~~
8 ~~[7th IEEE International Conference on Computer Vision, 2, 1150–1157, 1999.](#)~~
- 9 ~~[Lowe, D. G.: Distinctive image features from scale invariant keypoints. Intern. J. Comput.](#)~~
10 ~~[Vis., 60\(2\), 91–110, doi:10.1023/B:VISI.0000029664.99615.94, 2004.](#)~~
- 11 Lucieer, A., de Jong, S. and Turner, D.: Mapping landslide displacements using Structure
12 from Motion (SfM) and image correlation of multi-temporal UAV photography, *Prog. Phys.*
13 *Geog.*, 38, 1–20, doi:10.1177/0309133313515293, 2013.
- 14 Lucieer, A., Turner, D., King, D. H. and Robinson, S. A.: Using an unmanned aerial vehicle
15 (UAV) to capture micro-topography of antarctic moss beds, *Int. J. Appl. Earth Obs.*, 27, 53–
16 62, doi:10.1016/j.jag.2013.05.011, 2014.
- 17 Luhmann, T., Robson, S., Kyle, S. and Boehm, J.: *Close-Range Photogrammetry and 3D*
18 *Imaging*, 2nd edition, De Gruyter, Berlin, Germany, 683 pages, 2014.
- 19 Mancini, F., Dubbini, M., Gattelli, M., Stecchi, F., Fabbri, S. and Gabbianelli, G.: Using
20 Unmanned Aerial Vehicles (UAV) for High-Resolution Reconstruction of Topography: The
21 Structure from Motion Approach on Coastal Environments, *Remote Sensing*, 5, 6880–6898,
22 doi:10.3390/rs5126880, 2013.
- 23 Martin-Brualla, R., Gallup, D. and Seitz, S. M.: Time-lapse Mining from Internet Photos. in:
24 *IEEE International Conference on Computer Vision (ICCV)*, 2015.
- 25 ~~[Masiero, A., Guarnieri, A., Vettore, A. and Pirotti, F.: An ISVD-based Euclidian structure](#)~~
26 ~~[from motion for smartphones, Int. Arch. Photogramm. Rem. Sens., XL-5, 401-406, 2014.](#)~~
- 27 Meesuk, V., Vojinovic, Z., Mynett, A. E., and Abdullah, A. F.: Urban flood modelling
28 combining top-view LiDAR data with ground-view SfM observations, *Adv. Water Res.*, 75,
29 105–117, doi:10.1016/j.advwatres.2014.11.008, 2015.

- 1 Micheletti, N., Chandler, J. H. and Lane, S. N.: Investigating the geomorphological potential
2 of freely available and accessible structure-from-motion photogrammetry using a smartphone,
3 *Earth Surf. Proc. Landf.*, 40, 473–486, doi:10.1002/esp.3648, 2014.
- 4 Micheletti, N., Chandler, J. H. and Lane, S. N.: Structure from Motion (SfM)
5 Photogrammetry [Photogrammetric heritage. in:\(Chap. 2, Sec. 2.2\), In: Cook, S.J., Clarke L.E.
6 and Nield, J.M. \(Eds.\) Geomorphological Techniques, British Society of Geomorphology,
7 London](#), 2015.
- 8 Michoud, C., Carrea, D., Costa, S., Derron, M.-H., Jaboyedoff, M., Delacourt, C., Maquaire,
9 O., Letortu, P. and Davidson, R.: Landslide detection and monitoring capability of boat-based
10 mobile laser scanning along Dieppe coastal cliffs, Normandy, *Landslides*, 12(2), 403–418,
11 2015.
- 12 Mikhail, E., Bethel, J. and McGlone, J.: *Introduction to Modern Photogrammetry*, John Wiley
13 and Sons, Inc., New York, 479 pages, 2001.
- 14 ~~Mikolajczyk, K., Tuytelaars, T., Schmid, C., Zisserman, A., Matas, J., Schaffalitzky, F.,
15 Kadir, T. and Gool, L. Van.: A Comparison of Affine Region Detectors, *Intern. J. Comput.
16 Vis.*, 65(1-2), 43–72, doi:10.1007/s11263-005-3848-x, 2005.~~
- 17 Milan, D. J., Heritage, G. L. and Hetherington, D.: Assessment of erosion and deposition
18 volumes and channel change Application of a 3D laser scanner in the assessment of erosion
19 and deposition volumes and channel change in a proglacial river, *Earth Surf. Proc. Landf.*,
20 32(32), 1657–1674, doi:10.1002/esp.1592, 2007.
- 21 Monserrat, O. and Crosetto, M.: Deformation measurement using terrestrial laser scanning
22 data and least squares 3D surface matching, *ISPRS J. Photogramm. Rem. Sens.*, 63(1), 142–
23 154, doi:10.1016/j.isprsjprs.2007.07.008, 2008.
- 24 Morgenroth, J. and Gomez, C.: Assessment of tree structure using a 3D image analysis
25 technique—A proof of concept; *Urban Forestry and Urban Greening*, 13(1), 198–203,
26 doi:10.1016/j.ufug.2013.10.005, 2014
- 27 Nadal-Romero, E., Revuelto, J., Errea, P. and López-Moreno, J. I.: The application of
28 terrestrial laser scanner and SfM photogrammetry in measuring erosion and deposition
29 processes in two opposite slopes in a humid badlands area (central Spanish Pyrenees), *SOIL*,
30 1, 561–573, doi:10.5194/soil-1-561-2015, 2015.

- 1 Nolan, M., Larsen, C. and Sturm, M.: Mapping snow-depth from manned-aircraft on
2 landscape scales at centimeter resolution using Structure-from-Motion photogrammetry, *The*
3 *Cryosphere Disc.*, 9, 333–381, doi:10.5194/tcd-9-333-2015, 2015.
- 4 Nouwakpo, S. K., James, M. R., Weltz, M. A., Huang, C.-H., Chagas, I. and Lima, L.:
5 Evaluation of structure from motion for soil microtopography measurement, *Photogramm.*
6 *Rec.*, 29(147), 297–316, doi:10.1111/phor.12072, 2014.
- 7 Nouwakpo, S. K., Weltz, M. A. and McGwire, K.: Assessing the performance of Structure-
8 from-Motion photogrammetry and terrestrial lidar for reconstructing soil surface
9 microtopography of naturally vegetated plots, *Earth Surf. Proc. Landf.*, doi:10.1002/esp.3787,
10 2015.
- 11 Oppikofer, T., Jaboyedoff, M., Blikra, L., Derron, M.-H. and Metzger, R.: Characterization
12 and monitoring of the Aknes rockslide using terrestrial laser scanning, *Natural Hazards and*
13 *Earth System Sciences*, 9, 1003–1019, 2009.
- 14 Ouédraogo, M. M., Degré, A., Debouche, C. and Lisein, J.: The evaluation of unmanned
15 aerial system-based photogrammetry and terrestrial laser scanning to generate DEMs of
16 agricultural watersheds, *Geomorphology*, 214, 339–355,
17 doi:10.1016/j.geomorph.2014.02.016, 2014.
- 18 Passalacqua, P., Belmont, P., Staley, D. M., Simley, J. D., Arrowsmith, J. R., Bode, C. A.,
19 Crosby, C., DeLong, S. B., Glenn, N. F., Kelly, S. A., Lague, D., Sangireddy, H., Schaffrath,
20 K., Tarboton, D. G., Wasklewicz, T. and Wheaton, J. M.: Analyzing high resolution
21 topography for advancing the understanding of mass and energy transfer through landscapes:
22 A review. *Earth-Sci. Rev.*, 148, 174–193, doi:10.1016/j.earscirev.2015.05.012, 2015.
- 23 Pears, N., Liu, Y. and Bunting, P.: *3D Imaging, Analysis and Applications*, Springer, London,
24 499 pages, 2012.
- 25 Piermattei, L., Carturan, L. and Guarnieri, A.: Use of terrestrial photogrammetry based on
26 structure from motion for mass balance estimation of a small glacier in the Italian Alps, *Earth*
27 *Surf. Proc. Landf.*, 40(13), 1791–1802, doi:10.1002/esp.3756, 2015.
- 28 Pierrot-Deseilligny, M. and Clery, I.: APERO, an open source bundle adjustment software for
29 automatic calibration and orientation of set of images, *Intern. Arch. Photogramm. Rem. Sens.*,
30 38-5(W16), 269–276, 2011.

- 1 Pierrot-Deseilligny, M. and Clery, I.: Some possible protocols of acquisition for the optimal
2 use of the “Apero” open source software in automatic orientation and calibration, EuroCow
3 2012, Barcelona, Spain, (10pp), 2012.
- 4 [Pike, R. J., Evans, I. S. and Hengl, T.: Geomorphometry: a Brief Guide. In: Hengl, T. and
5 Reuter, H.I. \(Eds\) Geomorphometry: Concepts, Software, Applications. Developments in Soil
6 Science, 33, 1-28, 2008.](#)
- 7 Pollyea, R. and Fairley, J.: Estimating surface roughness of terrestrial laser scan data using
8 orthogonal distance regression, *Geology*, 39(7), 623–626, doi:10.1130/G32078.1, 2011.
- 9 Poropat, G.: Measurement of Surface Roughness of Rock Discontinuities. In Proc. of the 3rd
10 CANUS Rock Mechanics Symposium. Toronto, 2009.
- 11 Prosdocimi, M., Calligaro, S., Sofia, G., Dalla Fontana, G. and Tarolli, P.: Bank erosion in
12 agricultural drainage networks: new challenges from Structure-from-Motion photogrammetry
13 for post-event analysis, *Earth Surf. Proc. Landf.*, 40(14), 1891–1906, doi:10.1002/esp.3767,
14 2015.
- 15 Remondino, F., Spera, M. G., Nocerino, E., Menna, F. and Nex, F.: State of the art in high
16 density image matching, *Photogramm. Rec.*, 29(146), 144–166, doi:10.1111/phor.12063,
17 2014.
- 18 Rippin, D. M., Pomfret, A. and King, N.: High resolution mapping of supraglacial drainage
19 pathways reveals link between micro-channel drainage density, surface roughness and surface
20 reflectance, *Earth Surf. Proc. Landf.*, 40(10), 1279–1290, doi:10.1002/esp.3719, 2015.
- 21 Royan, M., Abellan, A. and Vilaplana, J.: Progressive failure leading to the 3 December 2013
22 rockfall at Puigcercós scarp (Catalonia, Spain), *Landslides*, 12(3), 585–595, 2015.
- 23 [Ruzic, I., Marovic, I., Benac, C. and Ilic, S.: Coastal cliff geometry derived from structure-
24 from-motion photogrammetry at Stara Baka, Krk Island, Croatia, *Geo-Mar. Lett.*, 34, 555–
25 565, doi:10.1007/s00367-014-0380-4, 2014.](#)
- 26 [Ryan, J. C., Hubbard, A. L., Box, J. E., Todd, J., Christoffersen, P., Carr, J. R., Holt, T. O.,
27 and Snooke, N.: UAV photogrammetry and structure from motion to assess calving dynamics
28 at Store Glacier, a large outlet draining the Greenland ice sheet, *The Cryosphere*, 9, 1-11,
29 doi:10.5194/tc-9-1-2015, 2015.](#)

- 1 Sanz-Ablanedo, E., Rodríguez-Pérez, J. R., Armesto, J. and Taboada, M. F. Á.: Geometric
2 stability and lens decentering in compact digital cameras, *Sensors*, 10, 1553–1572
3 doi:10.3390/s100301553, 2010.
- 4 Schaffalitzky, F. and Zisserman, A.: Multi-view matching for unordered image sets, or “How
5 do I organize my holiday snaps?”, *Computer Vision - ECCV 2002*, 2350, 414–431.
6 doi:10.1007/3-540-47969-4, 2002.
- 7 Shortis, M. R., Bellman, C. J., Robson, S., Johnston, G. J. and Johnson, G. W.: Stability of
8 Zoom and Fixed Lenses used with Digital SLR Cameras, *Intern. Arch. Photogramm., Rem.
9 Sens.*, XXXVI(5), 285–290, 2006.
- 10 Siebert, S. and Teizer, J.: Mobile 3D mapping for surveying earthwork projects using an
11 Unmanned Aerial Vehicle (UAV) system, *Automation in Construction*, 41, 1–14,
12 doi:10.1016/j.autcon.2014.01.004, 2014.
- 13 Smith, M. W., Carrivick, J. L., Hooke, J. and Kirkby, M. J.: Reconstructing flash flood
14 magnitudes using “Structure-from-Motion”: A rapid assessment tool, *J. Hydrol.*, 519, 1914–
15 1927, doi:10.1016/j.jhydrol.2014.09.078, 2014.
- 16 Smith, M. W. and Vericat, D.: From experimental plots to experimental landscapes:
17 topography, erosion and deposition in sub-humid badlands from Structure-from-Motion
18 photogrammetry, *Earth Surf. Proc. Landf.*, 40(12), 1656–1671, doi:10.1002/esp.3747, 2015.
- 19 [Smith, M. W., Carrivick, J. L. and Quincey, D. J.: Structure from motion photogrammetry in
20 physical geography, *Progress in Physical Geography*, 1-29, doi: 10.1177/0309133315615805,
21 2015.](#)
- 22 Snapir, B., Hobbs, S. and Waine, T. W.: Roughness measurements over an agricultural soil
23 surface with Structure from Motion, *ISPRS J. Photogramm. Rem. Sens.*, 96, 210–223,
24 doi:10.1016/j.isprsjprs.2014.07.010, 2014.
- 25 Snavely, N., Seitz, S. M. and Szeliski, R.: Photo Tourism : Exploring Photo Collections in 3D,
26 *ACM Transactions on Graphics*, 25(3), 835–846, 2006.
- 27 Snavely, N., Seitz, S. M. and Szeliski, R.: Modeling the World from Internet Photo
28 Collections, *Intern. J. Comput. Vis.*, 80(2), 189–210. doi:10.1007/s11263-007-0107-3, 2008.
- 29 Stöcker, C., Eltner, A. and Karrasch, P.: Measuring gullies by synergetic application of UAV
30 and close range photogrammetry — A case study from Andalusia, Spain, *Catena*, 132, 1–11,
31 doi:10.1016/j.catena.2015.04.004, 2015.

- 1 Stumpf, A., Malet, J.-P., Allemand, P., Pierrot-Deseilligny, M. and Skupinski, G.: Ground-
2 based multi-view photogrammetry for the monitoring of landslide deformation and erosion,
3 *Geomorphology*, 231, 130–145, doi:10.1016/j.geomorph.2014.10.039, 2014.
- 4 Sturzenegger, M. and Stead, D.: Close-range terrestrial digital photogrammetry and terrestrial
5 laser scanning for discontinuity characterization on rock cuts, *Eng. Geol.*, 106, 163–182,
6 doi:10.1016/j.enggeo.2009.03.004, 2009.
- 7 Tamminga, A. D., Eaton, B. C. and Hugenholtz, C. H.: UAS-based remote sensing of Wuvial
8 change following an extreme Wood event, *Earth Surf. Proc. Landf.*, 40(11), 1464–1476,
9 doi:10.1002/esp.3728, 2015.
- 10 Thomsen, L., Stolte, J., Baartman, J. and Starkloff, T.: Soil roughness: comparing old and
11 new methods and application in a soil erosion model, *SOIL*, 1, 399–410, doi:10.5194/soil-1-
12 399-2015, 2015.
- 13 Tonkin, T. N., Midgley, N. G., Graham, D. J. and Labadz, J. C.: The potential of small
14 unmanned aircraft systems and structure-from-motion for topographic surveys: A test of
15 emerging integrated approaches at Cwm Idwal, North Wales, *Geomorphology*, 226, 35–43,
16 doi:10.1016/j.geomorph.2014.07.021, 2014.
- 17 Torres-Sánchez, J., López-Granados, F., Serrano, N., Arquero, O. and Peña, J. M.: High-
18 Throughput 3-D Monitoring of Agricultural-Tree Plantations with Unmanned Aerial Vehicle
19 (UAV) Technology, *PLOS One*, 10(6), doi:10.1371/journal.pone.0130479, 2015.
- 20 [Triggs, B., McLauchlan, P., Hartley, R. and Fitzgibbon, A.: Bundle Adjustment - A Modern](#)
21 [Synthesis. In: Triggs, B., Zisserman, A. and Szeliski, R. \(Eds.\), *Vision Algorithms: Theory*](#)
22 [and Practice, Springer, Berlin, Germany, LNCS vol. 1883, 298–372, 2000.](#)
- 23 Turner, D., Lucieer, A. and de Jong, S.: Time Series Analysis of Landslide Dynamics Using
24 an Unmanned Aerial Vehicle (UAV), *Remote Sensing*, 7, 1736–1757,
25 doi:10.3390/rs70201736, 2015.
- 26 Ullman, S.: The interpretation of structure from motion. *Proceedings of the Royal Society B*,
27 203, 405–426, 1979.
- 28 Vasuki, Y., Holden, E. J., Kovesi, P. and Micklethwaite, S.: Semi-automatic mapping of
29 geological Structures using UAV-based photogrammetric data: An image analysis approach,
30 *Comput. Geosci.*, 69, 22–32, doi:10.1016/j.cageo.2014.04.012, 2014.

1 Westoby, M. J., Brasington, J., Glasser, N. F., Hambrey, M. J. and Reynolds, J. M.:
2 “Structure-from-Motion” photogrammetry: A low-cost, effective tool for geoscience
3 applications, *Geomorphology*, 179, 300–314, doi:10.1016/j.geomorph.2012.08.021, 2012.

4 Westoby, M. J., Glasser, N. F., Hambrey, M. J., Brasington, J., Reynolds, J. M. and Hassan,
5 M. A. A. M.: Reconstructing historic glacial lakeoutburst floods through numerical modelling
6 and geomorphological assessment: Extreme events in the Himalaya, *Earth Surf. Proc. Landf.*,
7 39, 1675–1692, doi:10.1002/esp.3617, 2014.

8 Woodget, A. S., Carbonneau, P. E., Visser, F. and Maddock, I. P.: Quantifying submerged
9 fluvial topography using hyperspatial resolution UAS imagery and structure from motion
10 photogrammetry, *Earth Surf. Proc. Landf.*, 40(1), 47–64, doi:10.1002/esp.3613, 2015.

11 Wu, C.: Towards linear-time incremental structure from motion, in: *International Conference*
12 *on 3D Vision - 3DV*, Seattle, WA, USA, 127–134, 2013.

13 Wu, C.: Critical configurations for radial distortion self-calibration, in: *IEEE Conference on*
14 *Computer Vision and Pattern Recognition (CVPR)*, 25 – 32. doi:10.1109/CVPR.2014.11,
15 2014.

16 Zarco-Tejada, P. J., Diaz-Varela, R., Angileri, V. and Loudjani, P.: Tree height quantification
17 using very high resolution imagery acquired from an unmanned aerial vehicle (UAV) and
18 automatic 3D photo-reconstruction methods, *Eur. J. Agron.*, 55, 89–99,
19 doi:10.1016/j.eja.2014.01.004, 2014.

20
21

1 | [Table 1. Nomenclature and brief definitions of image-based 3D reconstruction related terms](#)

2 | [Table 1. Nomenclature and brief definitions of image-based 3D reconstruction related terms](#)

Image-based 3D reconstruction	recording of the three-dimensional shape of an object from overlapping images from different perspectives
Computer Vision	algorithmic efforts to imitate human vision with focus on automation, amongst others, to reconstruct 3D scenes with methods of image processing and image understanding
Structure from Motion (SfM)	fully automatic reconstruction of 3D scenes from 2D images and simultaneous retrieval of the corresponding camera geometry in an arbitrary coordinate system
Photogrammetry	algorithmic efforts to determine 3D model coordinates and camera geometry focussing on accuracy and precise measurement in images
SfM photogrammetry	fully automatic reconstruction of 3D scenes from 2D images and camera geometry with option to set parameters for (photogrammetric) optimisation of accuracy and precision
Dense matching	increase of resolution of point clouds that model 3D scenes by pixel- or patch-wise matching in images of known intrinsic and extrinsic parameters
Stereo matching	reconstruction of object point through matching (in image space, Remondino et al., 2014) between two overlapping images
ulti-View-Stereo (MVS) matching	reconstruction of object point through matching (in object space, Remondino et al., 2014) from multiple overlapping images
Extrinsic parameters	exterior camera geometry comprising position (three shifts) and orientation (three rotations) of the camera projection centre
Intrinsic parameters	interior camera geometry comprising principle distance (distance between projection centre and image sensor), principle point (intersection of perpendicular from projection centre onto image plane) and distortion parameters (e.g. radial distortion)
Bundle adjustment (BA)	least-square optimisation to simultaneously solve for extrinsic (and intrinsic) parameters of all images; the term bundle correlates to rays that derive from 3D points, converge in corresponding projection centres and intersect with image sensor
Camera self-calibration	intrinsic camera parameters are included as additional unknowns into BA to solve for interior camera geometry
Ground Control Point (GCP)	in images clearly distinguishable point whose object coordinates are known to geo-reference surface model
Digital Elevation Model (DEM)	3D description of the surface in either raster (grid) or vector (mesh) format
Point cloud	quantity of points of 3D coordinates describing the surface within arbitrary or geo-referenced coordinate system, additional information such as normals or colours possible

3 |

[Table 2: Summary of non-commercial software tools beneficial for SfM photogrammetry processing and post-processing.](#)

<i>Software</i>	<i>Bundler</i>	<i>PMVS2</i>	<i>Apero+ MicMac</i>	<i>SfMToolkit</i>	<i>Meshlab</i>	<i>Cloud Compare</i>	<i>Sfm_georef</i>	<i>VisualSFM</i>	<i>SF3M</i>	<i>Photosynth</i>	<i>123D Catch</i>
<i>Type</i>	Open Source	Open Source	Open Source	Open Source	Open Source	Open Source	Freely-available	Freely-available	Freely-available	Free web service	Free web service
<i>Website</i>	http://www.cs.cornell.edu/~snavely/bundler	http://www.di.ens.fr/pmvs	http://logiciels.ign.fr/?Micmac	http://www.visual-experiments.com/demos/sfintoolkit	http://meshlab.sourceforge.net	http://www.danielgm.net/cc	http://www.lancaster.ac.uk/staff/jamesm/software/sfm_georef.htm	http://ccwu.me/vsfm	http://sf3map.csic.es	https://photosynth.net	http://www.123dapp.com/catch
<i>Operative system</i>	Linux Windows	Linux Windows	Linux Mac Windows	Windows	Mac Windows	Linux Mac Windows	Windows	Linux Mac Windows	Windows	Windows	Windows Mac
<i>Camera calibration</i>			x								
<i>Bundle adjustment</i>	x			x				x	x	x	x
<i>Bundle adjustment with GCPs</i>			x								
<i>Sparse 3D re-construction</i>	x		x	x				x	x	x	x
<i>Geo-referencing</i>			x				x	x	x		
<i>Dense 3D re-construction</i>		x	x					x	x		x
<i>Post-processing</i>			x						x		

*Advanced
cloud
processing*

x

x

1 [Table 3: Key developments of SfM photogrammetry towards a standard tool in](#)
 2 [geomorphometry](#)

3

4

key developments	authors
method introduction	James & Robson (2012), Westoby et al. (2012), Fonstad et al. (2013)
evaluation of accuracy potential	James & Robson (2012), Westoby et al. (2012), Castillo et al. (2012)
SfM with terrestrial images	James & Robson (2012), Westoby et al. (2012), Castillo et al. (2012)
SfM with UAV images	Harwin & Lucieer (2012)
application with mm resolution	Bretar et al. (2013), Snapir et al. (2014)
application covering km ²	Immerzeel et al. (2014)
mitigation of systematic errors (i.e. dome)	James & Robson (2014a), Eltner & Schneider (2015)
influence of image network geometry	Stumpf et al. (2014), Micheletti et al. (2014), Piermattei et al. (2015)
usage of Smartphone for data acquisition	Micheletti et al. (2014)
time-lapse implementation	James & Robson (2014b)
influence of scale	Smith & Vericat (2015)
comparing tools and cameras	Eltner & Schneider (2015)
synergetic usage of terrestrial and aerial images	Stöcker et al. (2015)
sub-merged topography	Woodget et al. (2015)
under water application	Leon et al. (2015)
reuse of historical images	Gomez et al. (2015)

5

6 [Table 2.](#)

1 [Table 4](#). Overview of the publication history divided in the main topics from 2012 until
 2 editorial deadline in [Sep/Nov](#). 2015. Several publications examined more than one topic
 3 resulting in a larger number of topics (~~number without brackets~~) than actual publications
 4 (number in brackets)- [in last row](#). IDs refer to the table in [appendix A1](#).

Topic	2012	2013	2014	2015	2016	ID	Total number of publications on the respective topic
Soil science/erosion	1	-	5	9	-	1, 2, 3, 5, 6, 9, 11, 18, 22, 23, 30, 31, 55, 60, 61	15
Volcanology	3	1	1	1	-	7, 15, 43, 44, 52, 54	6
Glaciology	-	-	4	6	-	12, 13, 14, 25, 27, 34, 37, 47, 51, 62	10
Mass movements	-	1	1	3	-	32, 35, 49, 56, 64	5
Fluvial morphology	-	1	5	3	1	4, 8, 16, 17, 21, 26, 29, 33, 37, 38	10
Coastal morphology	3	1	3	-	-	15, 20, 28, 36, 42, 50, 53	7
Others	1	2	8	5	-	7, 10, 17, 19, 24, 39, 40, 41, 45, 46, 48, 57, 58, 59, 63, 65	16
Topics (publications)	8 (6)	6 (6)	27 (25)	27 (27)	1(1)		69 (65)

5
 6
 7
 8
 9

- 1 Table 3: [Different perspectives/platforms used for image5: Data acquisition of all 62](#)
- 2 [reviewed studies](#). Table 4: [Parameters of a standard protocol for and error assessment protocol](#)
- 3 [for SfM photogrammetry](#); independent from individual study design.

<i>in the field:</i>					
target specifics	study area extent		ground control specifics	GCP measurement (total station, GPS, ...)	
	sensor to surface distance			GCP description	
	ground sampling distance			GCP number	
	target complexity			GCP accuracy	
camera specifics	camera name		image acquisition specifics	illumination condition	
	camera type (SLR, CSC, ...)			image number	
	lens type (zoom - fixed)			image overlap	
	sensor resolution			base (distance between images)	
	sensor size			network configuration (conv. - parallel-axis)	
	pixel size			perspective (aerial - terrestrial)	
	focal length				
			notes		
<i>at the office:</i>					
data processing specifics	SfM tool		accuracy assessment	registration residual	
	GCP integration (1-/2-staged)			reference type (LiDAR, RTK pts, ...)	
	output data type			reference error	
error ratios	relative error			error measure (M3C2, raster difference, ...)	
	reference superiority			statistical value (RMSE, std dev, ...)	
	theoretical error ratio				
			notes		

1 Figure captions

2

3 ~~Figure 1. Exemplary workflow of image-based 3D reconstruction: a) illustration of a micro-~~
4 ~~plot (1 m²), b) matched image pair with homologous points, c) reconstructed image network~~
5 ~~geometry with sparse point cloud, d) dense-matched point cloud, e) meshed DEM of micro-~~
6 ~~plot~~

7 Figure 1: Schematic illustration of the versatility of SfM photogrammetry.

8

9 Figure 2. Map of the research sites of all studies of this review.

10

11 Figure 3. Variety of ~~software~~SfM photogrammetry tools used in the ~~6265~~ reviewed studies.

12

13 Figure 4. Boxplots summarizing statistics: a) of the scale, of the study reaches (N: 56; ID 1-3
14 and 5-39 in Appendix A), b) the relative error ratio (calculated in regard to distance and
15 measured error, N: 54; ID 1-3, 5-12 and ~~distance~~14-39 in Appendix A), and ~~superior~~c) the
16 reference ~~ratio~~superiority (calculated in regard to measured error and reference error, N: 33;
17 ID 1-30 and 32-39 in Appendix A) of reviewed studies.

18

19 Figure 5. ~~Relationship between Performance of several error parameters in regard to the~~
20 camera to surface distance.a) Characteristics of measured error, ~~error ratio and distance and~~
21 relative error (N: 54; ID 1-3, 5-12 and 14-39 in Appendix A). For grey coloured points GCPs
22 are measured in point cloud (in total 9 times corresponding to the studies: ID 8, 11, 12, 28, 36,
23 37 in Appendix A) and for white points GCPs are measured in images (corresponding to the
24 remaining studies) for model transformation.

25

26 ~~Figure 6. Image-based 3D reconstruction performance of software considering basic and~~
27 ~~complex camera models.~~

28

29 ~~Figure 7. Influence of pixel size (and thus SNR) at the error ratio.~~

30

31 ~~Figure 8. No distinct relation between error and amount of images detectable. Different scales~~
32 ~~are considered with point grey scales.~~

33

34 ~~Figure 9. b) Superiority of the reference data. Superior reference ratio (N: 33), which is~~
35 ~~calculated as ratio between measured error and ~~accuracy~~error of the reference. Area based and~~

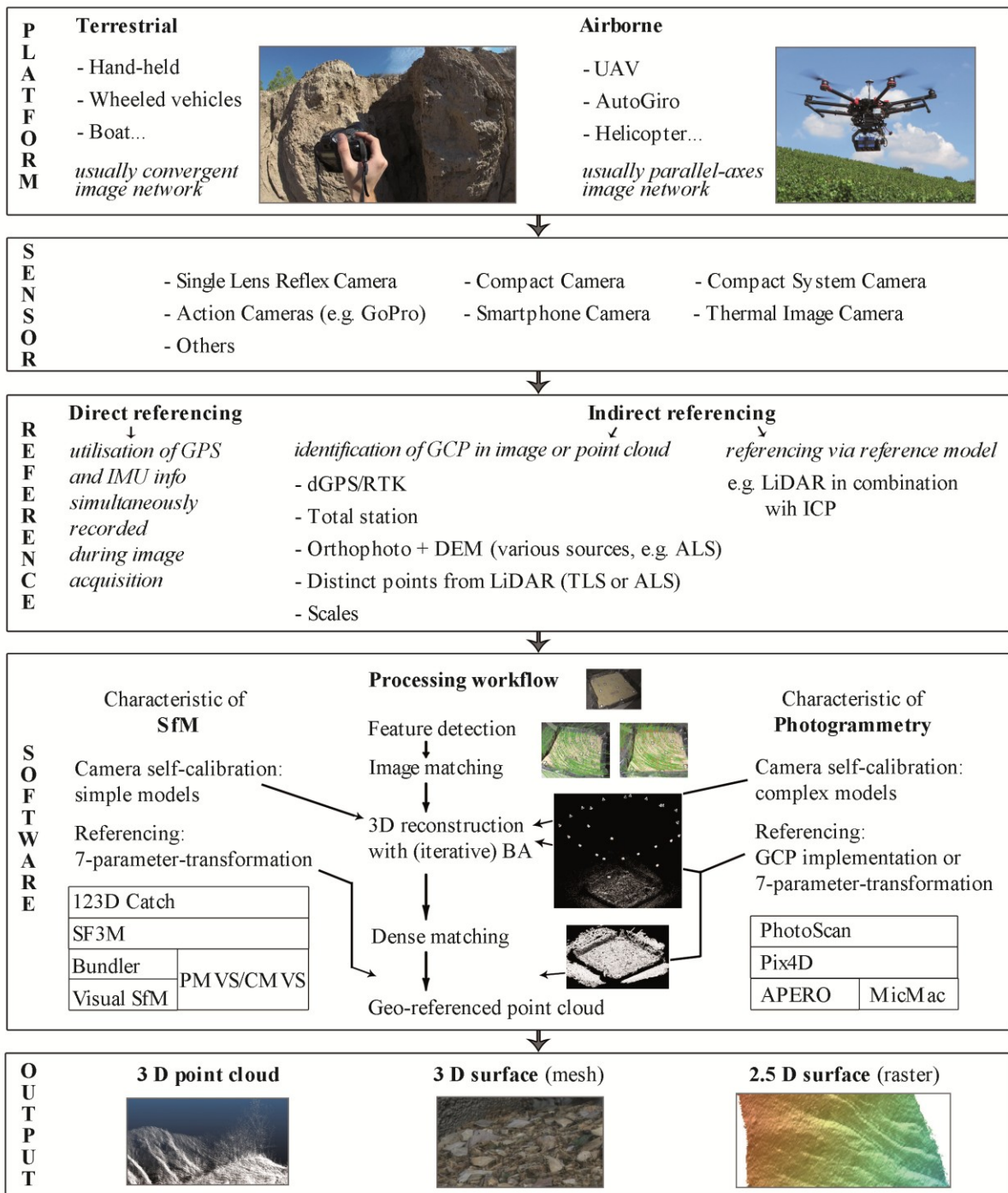
1 | ~~point based~~(ID 5-7, 12, 15, 17, 22, 25, 26, 30 and 32 in Appendix A) and point based (ID 2, 3,
2 | 8, 9, 20, 24, 28-30, 33, 35 and 37 in Appendix A) reference measurements are distinguished.

3 |
4 | ~~Figure 10. Ratio of the~~ c) Theoretical error ratio, considering the theoretical and measured
5 | ~~error displayed against distance,~~ to illustrate ~~image based 3D reconstruction~~SfM
6 | photogrammetry performance in field applications- (N: 23; ID 1-3, 8, 10-12, 15, 21, 22, 25,
7 | 26, 28-30 and 32 in Appendix A).

8 |
9 | ~~Figure 11: Schematic illustration of the versatility of SfM photogrammetry.~~

10

1 Figure 1:



2

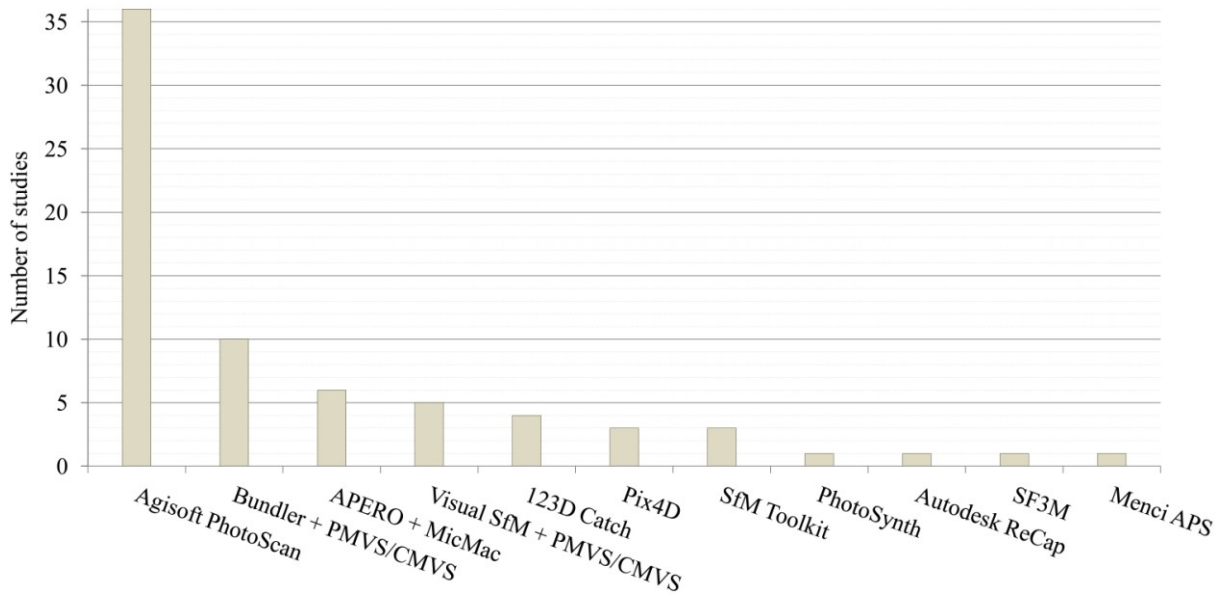
3

1 Figure 2:



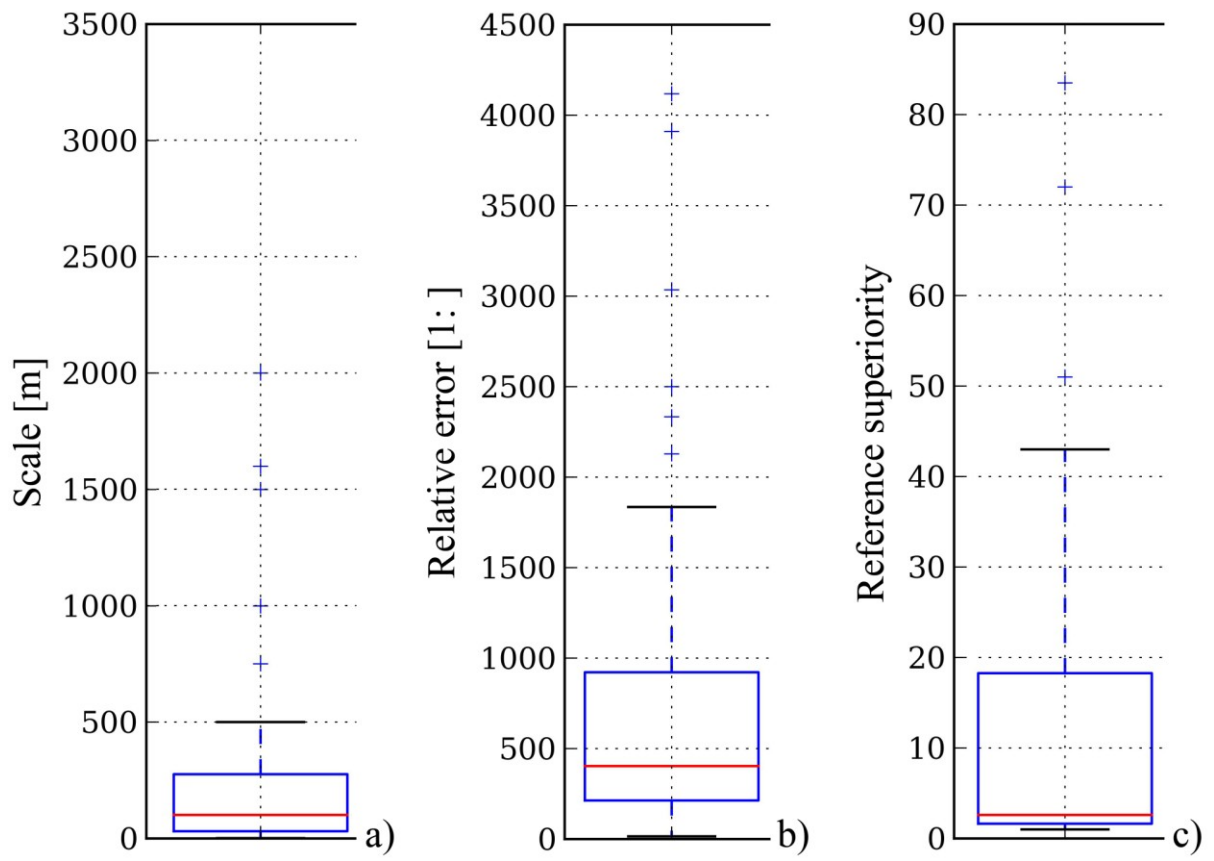
2
3
4
5

6 Figure 3:



7
8

1 Figure 4:



2

3

1 Figure 5:

